SuperCOSMOS Technical Manual

N C Hambly, L Miller

September 1997

Preface

This manual is an updated technical document describing various procedures for setting up, testing, evaluating and also developing the SuperCOSMOS system. It is based around the incomplete FrameMaker documents produced by Lance Miller (1996), but with significant changes due to new features of the machine (*e.g.* the new illumination unit and reinstallation of the slit in the imaging optics). It is intended that this document will be **the final** Technical Manual describing, in as much detail as possible, all the necessary set–ups and test procedures to ensure optimum machine performance.

Contents

List of Figures

List of Tables

Chapter 1

The SuperCOSMOS system

1.1 Introduction

The aim of this Chapter is to provide on overview of the components which comprise SuperCOSMOS, so that the reader may appreciate how the various sub–systems are related, and so that the reasons behind design decisions may be understood.

The principle behind SuperCOSMOS is very simple: light is shone through the photographic emulsion being measured, and the amount of transmitted light is measured by a CCD detector. The analogue output from the CCD is digitised and transfered to a transputer system where initial real–time data–processing is carried out, and then on to further post–processing on workstations. A scan of a plate is constructed by moving the plate through the light path; the physical movement is carried out by the Leitz PMM 654 co-ordinate measuring machine on which the plate is mounted. In practice, this process has to be carried out with high accuracy and speed.

1.2 Performance specification

The following performance criteria have been set as targets for SuperCOSMOS:

- Measurement area 0.5m square
- Absolute accuracy $< 1\mu$m, defined as the accuracy with respect to a perfectly uniform, rectilinear Cartesian co-ordinate system
- Repeatability $< 0.3\mu$m, defined as the largest variation in the absolute errors when measurements of the same plate taken on different days are compared: it is this performance criterion which is most important for obtaining accurate astronomical information.
- Dynamic range $> 10^4$, defined as the ratio of the highest transmission value measureable on a photographic plate to the lowest transmission measureable at a signal–to–noise ratio of unity
- Scattered light surface brightness $< 10^{-4}$ times the maximum measureable transmission value.
- Sampling interval 10μm

- Resolution (FWHM of point–spread function, including the effects of finite pixel size) 15μm
- Time needed to digitise a 14–inch Schmidt plate $<$ 2 hours
- Time needed to analyse the pixel data from a 14–inch Schmidt plate $<$ 2 hours

1.3 Imaging systems compared with 'flying–spot' systems

The COSMOS and APM plate measuring machines were both 'flying–spot' systems, in which a beam of light (either incoherent from a CRT as on COSMOS, or a laser spot as on APM) is rapidly scanned over a small area of plate, and the amount of transmitted light is measured. It is extremely difficult to meet the performance criteria outlined in Section 1.2 with a flying–spot system for two reasons. First, the location of the flying–spot is not precisely known as a function of time, resulting in small–scale positional errors. Second, because the light measurement system is diffuse it is susceptible to scattered light, especially any halo of scattered light around the spot. This problem was particularly acute on COSMOS.

A direct imaging system removes both of these problems. The imaging system can be made rigid, so that small–scall random position errors are eliminated (although systematic errors may remain) and because an image of the the emulsion is formed, and light which is transmitted through the emulsion contributes to forming a corect image of the plate, regardless of the origin of that light. Only scattered light introduced into the optical path between the emulsion and the detector can degrade the image quality, and with the correct choice of imaging system such light can be eliminated very effectively. Chapter 5 describes the imaging system set–up in more detail.

1.4 Scanning with SuperCOSMOS

The Leitz PMM 654 is a three axis co-ordinate measuring machine. Movement along the horizontal x– and y–axes is done by separate air–bearing granite blocks. The optical system is focussed on the plate using the vertical z–axis movement, which is mounted on the y–axis (note that there are two definitions of the co-ordinate systems in use: see Figure 1.1).

A photographic plate or film is mounted in a holder on the granite x–axis. Both the CCD imaging system above the plate and the illuminating system under the plate are mounted on a 'bridge' which wraps around the plate but which is not physically connected to it; the bridge is suspended from the y–axis. A plate is scanned in a series of lanes, by moving the x–axis and thus moving the plate through the optical path of the imaging system. The field–of–view of the imaging system is about 1.5cm; at the end of each x–axis, the x–axis is returned to its start position, the y–axis is stepped by an amount which defines the lane width (at present 11.52mm) and the next lane is scanned. The horizontal co-ordinate system defined in this way is illustrated in Figure 1.1. The co-ordinate system convention assumed by the SuperCOSMOS image analysis software has the origin at the top right; note that the intrinsic co-ordinate system used by the Leitz control computer differs from this, and hence the SuperCOSMOS control software makes a conversion between co-ordinate systems. These co-ordinate systems have become known as the 'Leitz' and 'SuperCOSMOS' co-ordinate systems. For example, the software translates between the two systems for a 14 inch Schmidt plate measurement via the transformations (units in mm) $X_{\rm Leitz} = 122.10 + Y_{\rm SuperCOSMOS}$; $Y_{\rm Leitz} = 422.93 - X_{\rm SuperCOSMOS}$.

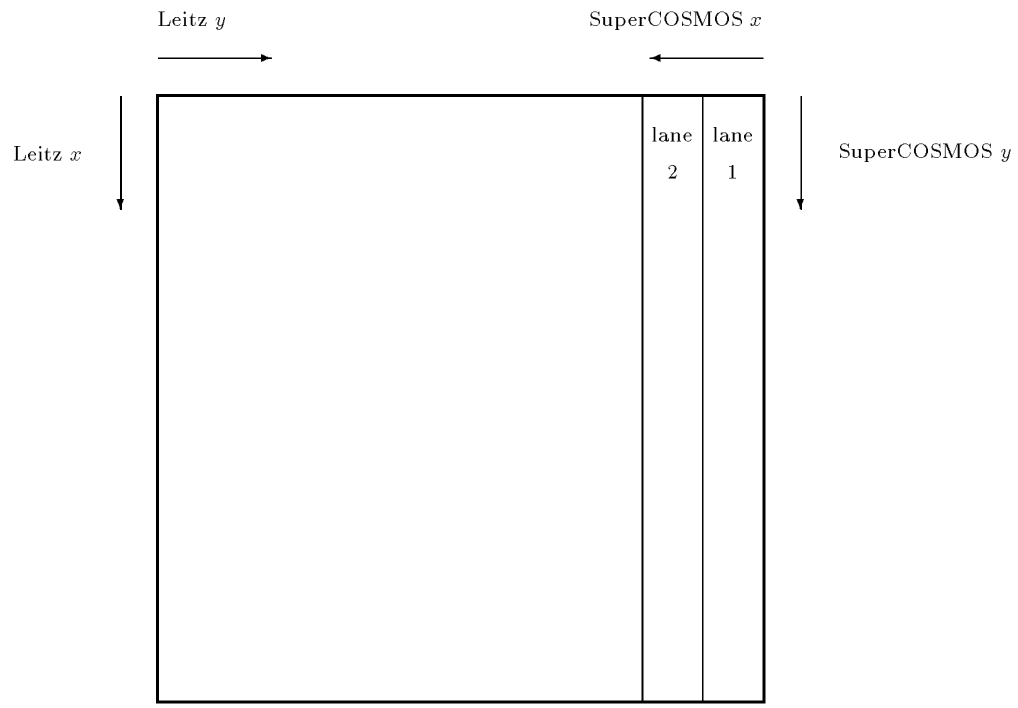

Figure 1.1: The Leitz and SuperCOSMOS co-ordinate system definitions. When viewing the machine from the loading bay doors, the Leitz origin is at the far left limit of travel of the xy axes.

During scanning of a lane, the table is simply driven at constant speed along the Leitz x–axis. In practice, of course, there are small variations in speed which, if not taken into account, would result in positional errors in the output, since if the CCD camera were read out at uniform time intervals, the table speed variations would result in non–uniform spacing of pixels in the final image. This is allowed for by linking the readout of the CCD to the table position. The table's position is measured by Moiré fringe gratings which produce two sinusoidal signals whose wavelength is 20μm, the two signals being out–of–phase by 5μm. A bistable flip–flop is switched every time one of those signals crosses zero (*i.e.* every 5μm); further electronics converts one edge of the resulting step function into a pulse. Pulses are thus delivered every 10μm of table movement. Those pulses are then used to trigger readout of the CCD; thus the pixel system perpendicular to the CCD is directly tied to the Leitz table co-ordinate system.

The positional accuracy of this method can be assessed by measuring the amount of light collected by the imaging system at each readout. Variations of $\pm 2\%$ in collected light are observed. This places an upper limit on the positional uncertainty: if those variations in collected light were entirely due to positional errors in the output from the gratings, with the table being driven at constant speed, then the largest positional error would be $\pm 2\%$, or 0.2μm. Some tuning of the grating output was required in order to achieve this, as the zero–crossings of the output sinusoidal signals were not initially set up to be equidistant. The zero–level was varied until the difference between successive readouts was minimised. This was measured by Fourier time–series analysis of the CCD output. The Fourier amplitude at the Nyquist frequency, corresponding to 10μm sampling, was minimised. If engineering work is carried out on the Moiré fringe gratings, this analysis will need to be repeated. In fact, the Fourier analysis showed that much of the variation in collected light was due to variations in table speed caused by mechanical imperfections in the drive system — clear mechanical resonances could be seen on the power spectrum of fluctuations. These were minimised as far as possible by a change of the drive motor from the original system.

1.5 Correction of errors in table position

Naturally, the apparent xy position of the table deviates somewhat from a perfectly uniform, rectilinear co-ordinate system. When in use as a co-ordinate measuring machine, the Leitz control system applies software corrections to the apparent positions in order to correct for this effect. Because of the high stability of the machine in its temperature controlled environment, it is expected that these corrections will remain systematic and fixed for long timescales ($>$ 1 year), and hence that software correction provides a viable means of obtaining an accurate measuring system. Measurement of NPL guage blocks confirmed that, with corrections in place, the large–scale absolute positional accuracy of the table (in the absence of the optical system and operating statically as a co-ordinate measuring machine) was indeed good to $< 0.3\mu$m. During a scan, however, these corrections cannot be applied to the machine, and hence systematic errors exist in the basic system. Some of these errors can be removed by applying new real–time position corrections during a scan (e.g. errors in Leitz y as a function of Leitz x); others can only be removed at the image processing stage (e.g. errors in Leitz x as a function of Leitz x; errors due to physical placement of pixels on the CCD). Chapter 6 deals with this subject in more detail.

1.6 The physical environment

SuperCOSMOS is housed in a special environment for two reasons. First, the machine room and plate preparation room are a class 100 cleanroom environment in order to reduce the amount of dust adhering to the emulsion and optical surfaces. This is particularly important in the measurement of films, when electrostatic attraction of dust is a major problem. Second, the machine room is temperature controlled in order to maintain the mechanical stability of the machine, and hence the astrometric accuracy. The high degree of repeatability required means that any physical expansion of mechanical subsystems due to temperature fluctuations must be limited to $< 0.3\mu$m. For glass components (such as the Moiré fringe gratings) this requries temperature stability of 0.1°K. As the absolute inaccuracies are larger than this, then in order for software to be able to remove systematic errors, that temperature stability must be maintained over long timescales as well as during the scanning of an individual plate. Temperature stability of the photographic plate is also vital, as expansion or contraction of the plate during the $\sim$ 2 hours needed per scan would cause differential shearing of the apparent position of stars which would be impossible to remove from the astrometric solution.

1.7 The CCD

The CCDs used on SuperCOSMOS are Loral–Fairchild CCD181 modules. They are linear devices with variable usable length. On SuperCOSMOS, 2048 pixels are read out. Each pixel is 10μm square, and the length of the original SuperCOSMOS CCD was measured in the laboratory as having its nominal length to an accuracy of one part in 10^3. On readout, the accumulated charge in each pixel is transferred into one of two shift registers which are located on either side of the light–sensitive portion of the device. One shift register is used for even–numbered pixels, the other for odd–numbered pixels. Separate pre-amp channels amplify the odd and even pixel signals before digitisation by the analogue–to–digital converter (ADC). The charge transfer time is 2μs, which is negligible compared with the integration time of 8ms, so the readout process results in essentially no dead–time during the scanning. The shift registers are continually clocked–out during an integration — a process which takes $2048 \times 0.002 = 4$ms. As this time is less than the integration time, the shift registers are empty when each integration is read out, except for 4ms of accumulated dark current in each pixel. The shift registers themselves have been coated with an opaque paint in order to prevent them responding to incident light during scanning.

The advantage of this system compared with, say, a two–dimensional device is that there is no dead–time associated with the readout, and hence the table can be operated in a continuous drift–scan mode. In addition, linear devices are cheap, they can be made cosmetically perfect (*i.e.* no dead pixels) and they have greater well–depths, leading to somewhat higher dynamic range. The time taken to scan a plate is almost independent of the number of pixels in the imaging detector, since the ultimate limit on the time needed is determined by the rate at which the CCD output can be digitised by the ADC. The ADC installed in the system digitises to 16–bit accuracy at a maximum rate of 2μs per pixel. To decrease the scan time further, a more complex system containing more ADCs, or an ADC with a faster clock speed would be required. Hence, the choice of a linear CCD does not limit the time needed to scan a plate; moreover it has many advantages over a two–dimensional array.

1.8 The imaging system

The Leitz table descibed in Section 1.4 is one key component in the design of a measuring machine with the required accuracy. The second key component is the system which images the emulsion onto the detector. This has to be of high image quality (as measured by the 'modular transfer function', or MTF, and by the amount of scattered light) and free from any type of distortion which can vary either randomly due to mechanical defects, or systematically with table position.

The design chosen is based around a commercially–available telecentric lens. A telecentric lens has a stop placed so that only rays parallel or nearly parallel to the optical axis are allowed to form an image. This means that the magnification of the image formed is insensitive to the distance between the object (*i.e.* the emulsion) and the lens. Since we require positional stablity of $< 0.3\mu$m in the image plane, the system is required to have a magnifiaction which is fixed to about one part in 10^5. Without a telecentric lens, for an object–lens distance of 20cm, this would place an upper limit on the amount of variation which could be allowed in the object–lens distance of 2μm! With the current telecentric lens, the amount of allowed variation is $\pm 25\mu$m, comparable to the depth–of–field required to obtain an acceptable MTF.

The telecentric lens system also has the advantage that it rejects off–axis scattered light very efficiently, to the extent that scans taken with the chamber lights left on show no discernible degradation in image quality from scan taken with the chamber darkened. The disadvantage of this, however, is that the effective range in optical density of the system is reduced. This arises because much of the light which is transmitted through a dark photographic emulsion is scattered off–axis. A diffuse densitometer can collect that light, but the SuperCOSMOS imaging system is highly specular, and the measured transmission of dark emulsions is much lower than would be measured by a diffuse densitometer. The ratio of specular–to–diffuse densities is called the Callier Q–factor, and has a value of $Q \sim 1.6$ for a IIIaJ emulsion measured on SuperCOSMOS. Hence an emulsion with a diffuse optical density of 2 has a SuperCOSMOS density of 3.2, at which the amount of light measured is a factor 16 times less than would be expected from the diffuse density value.

1.9 Focussing

As plates have different thicknesses, and because they sag under gravity when held horizontally and clamped along their edge, it is necessary to focus the imaging system on the emulsion and to continually vary the z–axis position as a function of xy position on the plate. This is done by first determining the vertical position of the emulsion for the plate about to be measured on a 6×6 grid of locations over the plate. A bivariate Chebyshev polynomial surface incorporating terms up to fifth–order is then fitted to those data, and the coefficients of the surface fit are loaded into the transputer control system. When scanning, the transputer control software uses those coefficients to calculate the z–axis position accordingly. Because of limitations on the rate of data transfer along the Leitz RS232 control line, these updates are only made every 3.75cm of x–axis movement.

The initial determination of the height of the emulsion is carried out by taking data with the table static at a series of different z–axis positions. Those data are analysed by measuring the sum of the absolute value of the difference between adjacent pixel values, for all pixels within some specified range. This is a measure of the granularity of the emulsion, and should be a maximum when the emulsion is in focus. The depth of field of the imaging system is about $\pm 50\mu$m; *cf.* the amount of plate tilt/sag of up to 500μm.

1.10 The illumination system

The SuperCOSMOS illumination system is based around high surface brightness, high stability Hamamatsu xenon arc lamps. The electrode construction of the lamps, coupled with the high stability power supply unit (also supplied by Hamamatsu) provide sufficient light to yield background counts of 10000 to 20000 ADU from the CCD/ADC for plates having background diffuse densities typical of the darker survey grade Schmidt plates in the UKSTU plate collection (lighter plates require varying amounts of ND to be introduced into the beam to avoid CCD saturation — this is provided for by an ND filter wheel — see Section 2.5). An ellipsoidal mirror gathers and focusses the arc lamp light; a 45° 'cold mirror' reflects the visible light into collimating optics, at the same time allowing the thermal infrared to pass out of the main beam. A two–stage convex lens system collimates the beam, whereupon a further near–infrared filter and high band pass filter yield $\sim$ 100nm bandwidth of light centred at $\sim$ 550nm (the green part of the visible spectrum, for which the optics are optimised). The near infrared block is needed to filter out two particularly bright spectral lines, between 800nm and 900nm where the photoelectric devices are most sensitive, from the xenon arc lamp which would otherwise severely degrade the performance of the imaging system. A 45° clear glass piece extracts a $\sim 1\%$ sample of the whole collimated beam into the reference beam, where a diffuser screen and microscope objective feed the sample into a small diameter 10m long fibre–optic bundle. This provides the reference channel signal (see Section 4.4). A further convex lens pair in the main beam focus the light through the ND filter position onto a gimble mounted, 7mm diameter, 10m long fibre–optic bundle which supplies the main light source to the machine (the illumination unit is outside the machine chamber in order that the high power dissipation of the former does not disturb the temperature stability of the latter). All optical components from the arc lamp to the face of the main fibre bundle are air–cooled by a fan. The filter wheel is software controlled via a Digiplan stepper motor and control unit; the filter wheel itself is datumed via a Hall–effect switch supplied by an RS 5V PSU. The complete illumination unit was designed and assembled by Light Support Limited of Reading, Berkshire. Small modifications to aid in the set–up and alignment of the unit were made by John Harris and Nigel Hambly; these are described in a separate document which also details procedures to align the components and optimise the throughput. Section 5.4.3 describes how to change the lamp. Note that the unit's power supply and fan are connected through a safety 'lock–in' unit which will not allow the lamp to be on without the fan being on; moreover if the lamp housing is hot the fan cannot be swithed off (obviously this safety unit will not work in the event of mains power failure).

At the machine end, the two fibre bundles are attached to the bridge. The small diameter reference fibre ends in a ferrule which is held in the reference PCB, where a photodiode monitors the reference level. The large diameter main fibre bundle enters the slit projection unit, where a condensing lens, optical slit, 45° mirror and projecting lens illuminate a strip in the object plane. A further lens images this strip onto the CCD. Section 1.8 gives more details of the telecentric illuminating/imaging lens pair. The optical slit position is focussed via a slide driven by a stepper motor under software control — Section 5.3 describes the set–up of the slit.

Chapter 2

Engineering tests

2.1 Introduction

It is frequently useful to operate SuperCOSMOS in a low–level engineering mode in order to diagnose faults, carry out detailed inspection of data, or test new developments to the system.

All commands and data are communicated through the transputer system. SuperCOSMOS software engineer Jim Herd (*J.T.Herd@hw.ac.uk*) has written a suite of low–level C programs which can be commanded on the workstation, and which instruct the transputer system to carry out individual functions. Those programs may in turn be called from shell scripts running on the workstation. All the basic functions of SuperCOSMOS can be accessed in this way, including data acquisition and system control. More sophisticated operations such as multiple lane mapping do not currently have equivalent low–level programs or scripts set up, although it would in principle be possible to do this. The graphical user interface (GUI), which is launched by typing

```
cosaxp0> cosgui &
```

provides high–level control for routine plate measurements (see the SuperCOSMOS Operator's Manual for more details). This Chapter describes how to operate the system in the low–level mode and how to use existing scripts and programs for collecting and analysing test data. If the machine is handed over to an engineer with the GUI still in operation, check that the last job has transferred before clicking on 'kill tasks' and 'exit'.

2.2 Location of files

2.2.1 Command files

Programs written by Jim Herd are in directory `/home/scosdev/<v...>/source/t_tools/*.c`; some basic shell scripts are held in the system `bin` directory `/home/scosdev/v<...>/bin`, where `<v...>` is used to denote the current software version number (*e.g.* v033). These include scripts for obtaining dark current data and flatfield data and are themselves used by the higher level SuperCOSMOS operating system (*i.e.* the GUI). Shell scripts and executables written by Lance Miller which are used for engineering tests are in directory `/home/scosdev/<v...>/lam/bin`. In the case of executables, the source code is in directories `/home/scosdev/<v...>/lam/c` or `/home/scosdev/<v...>/lam/for`. Further scripts and executables written by Nigel Hambly are in /home/nch/scos/scripts and /disk1/nch/scratch/bin/osf; in this case FORTRAN source codes are held in /home/nch/scos/fortran.

At present, directory paths containing lam or nch are not included into the path of either scos or scosdev users, and hence if access to these files is needed by name alone with no path, the directories should be explicitly added to the environment variable PATH, *e.g.*:

```
cosaxp0> setenv PATH {$PATH}:/home/scosdev/v033/lam/bin:
         /home/nch/scos/scripts:/disk1/nch/scratch/bin/osf
cosaxp0> where shortdarktime
/home/scosdev/v033/lam/bin/shortdarktime
```

2.2.2 System correction files

Files such as the linearity corrections, geometry corrections, flatfields and dark frames are stored in the machine directory /sdata/scos/machine. A typical directory list is as follows:

```
black                 # time dependent bias (‘T black’)
black9709291040       # old black file renamed when new one derived
ccd.linearity         # non-linearity look-up table for the CCD
ccd.linearity.old     # old CCD linearity LUT
dark                  # bias frame used by real-time correction software
dark9709291040        # old bias frame
fine.sdf              # fine focus data structure
flat2                 # flatfield frame for filter wheel position 2
flat29709291056       # old flatfield frame
linear.linearity      # linear LUT used when deriving linearity data
ref.linearity         # non-linearity LUT for the reference channel
residual.corrns       # offline positional correction coefficients
residual_Full.corrns  # current full correction coefficients
residual_Zero.corrns  # coefficient file to switch off offline corrections
rough.sdf             # rough focus map data structure
rough_origs.sdf       # rough focus map for 1mm (sagging) plates
table.corrns          # scan-time correction LUT for Leitz geometry errors
xpoly.tcl             # scan-time correction coefficients
yoptdist.corrns       # offline coefficients for optical distortion
zero.corrns           # zero LUT for switching off table.corrns
zx.corrns             # scan-time LUT for errors as a function of Z
```

These files have a mixture of formats, and therefore different methods must be used to inspect their contents. Detailed descriptions of their derivation are provided later in this document.

2.3 File formats and displaying

2.3.1 Linearity correction files

These are in the form of a lookup–up table (LUT) of floating point values, one for every possible input integer produced from the ADC, *i.e.* 32768 values in the range 0 to 32767. There is no header information. To inspect:

```
cosaxp0> od -f ccd.linearity | more
```

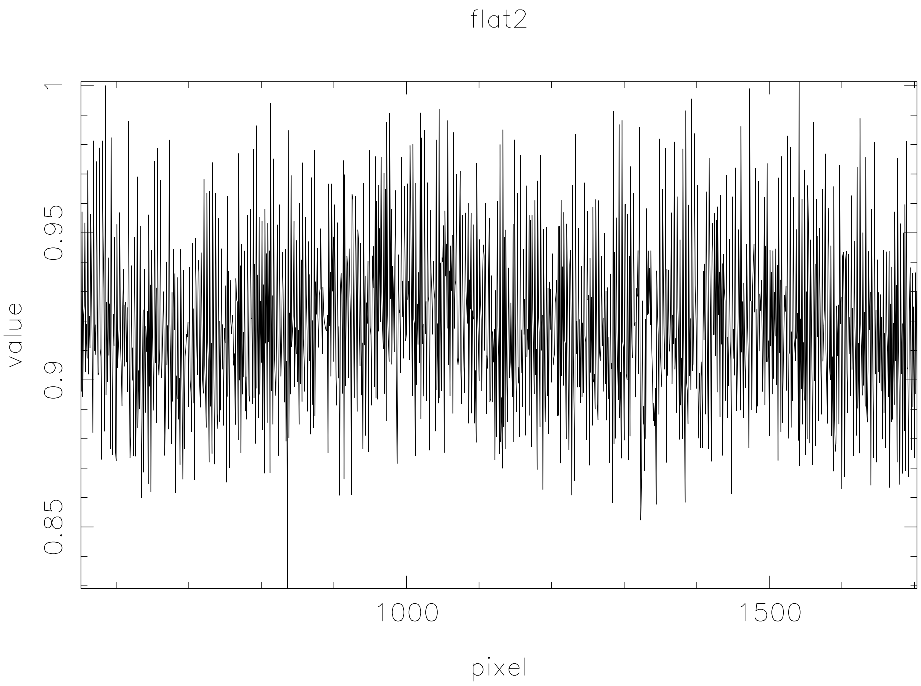

Figure 2.1: A typical flatfield, obtained at filter position 2 and displayed using **flatfieldplot**.

2.3.2 Focus data structures

These are STARLINK data structures. To inspect:

```
cosaxp0> hdstrace fine
```

2.3.3 Flatfield, dark & black frame files

These are the form of a floating point number, one for each of the 2090 pixel values. Inspect as for the linearity LUTs, or alternatively graphical display of the data values may be made as follows. For a line plot of flatfield or dark frame values:

```
cosaxp0> flatfieldplot <file> <start_pixel> <end_pixel> <plotting_device>
```

e.g.:

```
cosaxp0> cd /sdata/scos/machine
cosaxp0> flatfieldplot flat2 552 1703
 Graphics device/type (?  to see list, default xwindows):
xwindows
cosaxp0>
```

– which displays the currently used portion of the CCD (1152 pixels) – see Figure 2.1. The ratio of two corrections files (useful for monitoring stability, for example) can be obtained thus:

```
cosaxp0> flatcompare <1st flat> <2nd flat>
```

e.g.:

```
cosaxp0> cd /sdata/scos/machine
cosaxp0> flatcompare
 1st flatfield filename ? flat29709100900
 2nd flatfield filename ? flat29709110900
 reference values differ by fraction    -0.1207E+00
 Graphics device/type (?  to see list, default xwindows):
xwindows
cosaxp0>
```

– which displays two flatfields taken through clear air on consecutive days.

2.3.4 Geometry correction files

LUTs are generally binary files of double–precision values (`table.corrns, zx.corrns`). To inspect:

```
cosaxp0> od -F table.corrns | more
```

Files of coefficients are generally in ASCII format (*e.g.* `residual.corrns, yoptdist.corrns`). To inspect:

```
cosaxp0> more xpoly.tcl
```

2.3.5 Engineering data files

Engineering data may be acquired, stored temporarily in transputer memory, and then transfered to the workstation for analysis or inspection. Up to 3000 scans may be transfered in this way. All the existing engineering shell scripts use this mode of data collection. The file format comprises a header of 4180 bytes. The scan length is stored as a 4 byte integer in the first word. This is normally 2090 pixels. The number of scans is stored as a 4 byte integer in the second word. This should be in the range 1–3000. Scans of data are then stored sequentially as 2 byte integers. A few utilities exist for inspecting the values in these files as grey–scale images or as line plots (Section 2.9).

2.4 Startup

2.4.1 Logging in and initialising the software

If the control workstation `cosaxp0` is not already logged onto under username 'scos' then log in under that username (see one of the operators or scientists for the password). Then, the software suite is initialised by typing

```
cosaxp0> v033
```

where 33 is the current version number of the software (this is periodically incremented when software changes are made – if the above command does not work then increase the number by one and try again).

2.4.2 Resetting the Leitz computer and transputers

If the table encounters an error (*e.g.* air pressure out of range or table driven to position limits) the Leitz computer will need to be reset. This will also be necessary if a communication between the Leitz computer and the transputers has been interrupted, either by an error or due to user intervention.

The simplest way to reset the computer is to press the red reset button on the front panel. Software reset may be achieved via the following set of commands:

```
cosaxp0> loadsys
cosaxp0> writeio 26 1 7 0
cosaxp0> writeio 26 1 7 1
cosaxp0> writeio 26 1 7 0
cosaxp0> loadsys
cosaxp0> getdataarea 25 2 0 junk
cosaxp0> autozero
```

It is possible to check if the Leitz computer is in an error state by inspecting the diagnostic LEDs at the top right, behind the Leitz front panel. There are two columns of three red LEDs. Only the lower right LED should be illuminated. Also behind the front panel are three boards which drive the three axes on the table. Each board should have a flashing LED indicating correct operation. In the event of a fault with the table drive system the appropriate LED will stop flashing. Note that under normal operating conditions the large red knob with white arrows marked should be pulled out to enable the table drive (a yellow light should be on, indicating that the drives are enabled).

2.4.3 Resetting the transputers

After a Leitz computer reset, or if an error has been generated within the transputer system, the transputers will need to be reset. This is done as follows:

```
cosaxp0> loadsys
```

This command bootstraps the transputers, datums the ND filter wheel etc., *i.e.* it generally prepares the system for use. There are four sets of three vertical LEDs on the transputer boards enscribed A,B,C and D (reading right to left) inside the lockable unit in the rack next to control Alpha workstation (cosaxp0) in the computer room. Beneath this cabinet, there are three sets of five vertical LEDs on the TAXI receiver where the orange fibre–optic data link connects the transputer system to the camera board. Under normal operating conditions, no LEDs should be illuminated on the transputer boards, while the top LEDs should be illuminated on the TAXI receiver boards.

2.4.4 Autozeroing the table

If the Leitz computer has been reset, it will be necessary to datum the table before any further movement is possible (*e.g.* as in Section 2.4.2 above). This is accomplished by the command:

```
cosaxp0> autozero
```

Note that since `autozero` datums the table, any absolute positional reference is lost. On the z-axis in particular, there is a zero–point uncertainty of $\sim 100\mu$m when an `autozero` command is issued. Thus, for example, a focus measurement for a particular plate must be redone – a previous focus measurement will, in general, no longer be valid.

2.4.5 Disabling the Leitz geometry corrections

The Leitz table control computer is supplied with ROMs containing LUTs for the geometry errors of the xyz co-ordinate system of the table. Because these were never remeasured by Leitz once the machine was complete, and because it is necessary to be able to monitor and correct these systematics (see Chapter 6), the original corrections should always be turned **off**. This is done explicitly by the high–level control, but not by `loadsys`. To disable the Leitz corrections:

```
cosaxp0> setparam 25 0 191
```

The last parameter may also take the values 190 (for enable) and 192 (for hold).

2.4.6 Loading the system scan–time corrections

It is essential to reload appropriate system corrections before data are acquired. These include the linearity corrections for the CCD and reference photodiode, dark current values and flatfield values. Executing the command:

```
cosaxp0> loadcorrections flat<n>
```

loads all four corrections, taking the dark and linearity frames from the default filenames described in Section 2.2.2 and the flatfield filename appropriate to the filter wheel position `<n>` as specified, also from the machine directory.

If any of these corrections files are not available, or if they are out of date, then new corrections should be generated and loaded. Note that new linearity corrections, if needed, should always be loaded **before** new dark and/or flatfield corrections are derived. In this case `loadcorrections` should be used with any convenient choice of dark and flatfield frames; these should then be replaced by the filenames of new corrections once they have been derived. Chapter 4 describes the various scan–time corrections in the system, and the procedures for deriving new sets of correction data.

2.5 Setting the light level

The light level reaching the CCD may be controlled by selection of an ND filter (in the filter wheel contained in the illumination unit in the control room) as follows:

```
cosaxp0> movewheel <position> <offset> <speed>
```

At present, `<offset>` should be 0, and `<speed>` 20. Filter choice currently goes from ND2.2 at position 1 down to clear at position 16. Position 0 is blank, and blocks the light path to the CCD (*e.g.* for use when deriving a dark frame – see Section 4.2.4). Table 2.1 details the currently available ND steps. Hence, to set the illumination level to the 'clear air' setting:

```
cosaxp0> movewheel 2 0 20
```

Filter No.	Filter Density
0	Blank (*i.e.* ND= ∞)
1	2.2
2	2.0
3	1.8
4	1.6
5	1.4
6	1.2
7	1.1
8	0.88
9	0.71
10	0.65
11	0.51
12	0.46
13	0.27
14	0.22
15	0.14
16	Clear

Table 2.1: Available ND steps in the filter wheel

2.6 Moving the slit

An optical slit is provided in the projection box on the SuperCOSMOS bridge assembly to illuminate the CCD strip only, and to cut down the extraneous light levels. This is necessary to keep scattered light to a minimum, but more importantly to limit the light available to diffraction in the imaging lens (the Airy disk). Without the slit, the dynamic range of the machine would be limited to $\sim$ 1.6D specular (or $\sim$ 1.0D diffuse for a IIIaJ emulsion). The slit position must be refocussed from it's clear air focus point when any thickness of glass is introduced in the object plane (*i.e.* glass–backed photographic plates). A command is provided to move the slit:

```
cosaxp0> slitmov <x> <speed>
```

where `<x>` is the plate thickness in millimetres and `<speed>` should be 100. A lower level command moves the slit in terms of steps of the motor slide:

```
cosaxp0> moveslit <steps> <speed>
```

where `<steps>` is the number of steps required and `<speed>` is as before. For example:

```
cosaxp0> moveslit 0 100
```

will datum the slit whereas

```
cosaxp0> slitmov 0 100
```

will move the slit to the clear–air focus position (having first datumed — for the sake of safety and accuracy, any high level slit move is preceeded by a datum command). Section 5.3 deals with the detailed procedure for alignment and determination of the focus parameters of the slit and gives more details on the software limits set up to avoid the slit carriage impacting with the condenser lens in the slit projection unit. Note that the software is set up so that the operator does not need to know the focus positions in terms of motor/slide steps — all the necessary movements for plate measurements can be achieved with the command `slitmov` and/or with the GUI.

2.7 Positioning the table

It is sometimes necessary to position the scanning head over a certain part of a plate or test chart. There are two commands pertaining to xyz motion under software control:

```
cosaxp0> readpos
```

This command reads the current table position (useful if you may want to return to this exact location after having moved the table).

```
cosaxp0> absmov <axis option> <xpos> <ypos> <zpos>
```

This command will execute an 'absolute move'. The position values are in units of mm; the axis option is a three–character string specifying which of the three axes to move. Characters `xyz` command motion of those axes; a minus sign indicates no change to that particular axis, *e.g.*:

```
cosaxp0> absmov x-z 300. 200. 395.5
```

would move the x-axis to position 300.0 mm, the z-axis to position 395.5 mm and leave the y-axis unchanged.

2.8 Obtaining test data

First, the precise mode of operation must be considered: do you want a map of data obtained by scanning the table, or a set of data obtained with the table stationary? Do you want all the corrections enabled? If you want to scan the table, do you want to use the normal operating speed (1.25 mm/sec), or to scan at a different rate? In some cases you may wish to create a custom script file by editing an existing one in order to obtain the data that you want. In many cases an existing script will serve. Of these, the most useful are:

```
cosaxp0> locate <no. of scans> <file>
```

– which makes a small map (up to 3000 scans, or 30 mm) with all corrections enabled at normal scanning speed; and:

```
cosaxp0> static <file>
```

which takes 10 scans without table motion, all corrections enabled, leaving the filter wheel set at whatever the current value is. Other scripts exist for taking data – for example, with scan corrections turned off. Look in the directories containing the shell scripts:

```
cosaxp0> ls ~scosdev/v033/lam/bin
...
cosaxp0> ls ~nch/scos/scripts
...
```

2.9 Displaying test data

2.9.1 Grey–scale maps

The program `displaysc` may be used to produce a grey–scale map of engineering data, and to inspect individual pixel values:

```
cosaxp0> displaysc
name of data file ?
scan length us      2090 : range of pixel numbers to use ?   # default is all
number of scans is  3000 : range of scan numbers to use ?    # default is all
Plot device  [xwin] (? for help) xwindows
use left mouse button to read cursor value,
use right mouse button to exit
```

2.9.2 Line plot of one or more scans

A cross–section through a set of engineering data may be plotted using `pixelplot`, plotting pixel values against pixel number. If a range of scans are specified, then those scans are averaged to make a single plot:

```
cosaxp0> pixelplot
name of data file ?
scan length us      2090 : range of pixel numbers to use ?   # default is all
number of scans is  3000 : range of scan numbers to use ?    # default is all
Plot device  [xwin] (? for help) xwindows
```

2.9.3 Time plot of one or more pixels

A plot of pixel value against scan number (or, equivalently, against time) can be made using `timeplot`. If a range of pixel numbers are specified, the values are averaged to produce a single plot:

```
cosaxp0> timeplot
name of data file ?
scan length us      2090 : range of pixel numbers to use ?   # default is all
number of scans is  3000 : range of scan numbers to use ?    # default is all
plot distance (d) or time (t) ? [default time]
INVALID ANSWER: assuming TIME plot
time interval between scans (secs) ? [default 1] 0.008
Graphics device/type (? to see list, default xwindows):
```

2.10 Analysing engineering data

2.10.1 Simple statistics

Mean and RMS fluctuations about the mean can be calculated using `mean`:

```
cosaxp0> mean
 name of data file ? lamp.dat
 scan length of this file is  2090
 give start & end pixel numbers for mean: 12 15
 this file contains      3000 cans
 give start & end scan numbers for mean: 1 3000

    mean           rms deviation   error of mean
     4967.02            8.19             0.15
```

2.10.2 Arithmetic operations

Frames of engineering data may be subtracted using `subtract_2dframe`:

```
cosaxp0> subtract_2dframe
...
```

2.10.3 Power spectrum analysis

A one–dimensional power spectrum of the time variations in engineering data may be calculated and plotted using `timefft`:

```
cosaxp0> timefft
...
```

2.10.4 Bit maps/pixel value histograms

To check for accurate ADC coding, for example, use `bitmap`:

```
cosaxp0> ~scosdev/v033/lam/bin/bitmap # NB: explicit path given due to conflict
                                      # with existing OSF command name
...
```

Pixel value histograms can be plotted using `enghistplot`:

```
cosaxp0> enghistplot
...
```

2.11 The system error codes

If the system detects an error (for example, if the table has developed a fault – *e.g.* air pressure out of range), then an error code will be generated. The error codes are as follows (list taken from `/home/scosdev/v033/include/supercos.h`):

```
 /* System Errors.
 * =============
 *
```

```
 * ALL errors to have negative values.
 *
 */
#define   OK                0
#define   FAIL             -1
#define   FAIL_TIME_OUT    -2
#define   FILE_ERROR       -3
#define   BAD_UNIT             -100
#define   BAD_CHAN_INIT        -101
#define   BAD_PROC_INIT        -102
#define   BAD_SCAN_LEN         -103
#define   BAD_NOS_SCANS        -104
#define   BAD_SCAN_PERIOD      -105
#define   OVERRUN              -106
#define   TABLE_STOPPED        -107
#define   FAIL_10um_STREAM     -108
#define   FAIL_TAXI_BUSY       -109
#define   COMMAND_IN_PROGRESS  -110
#define   ERROR_IN_LAST_READ   -111
#define   FAIL_NO_DATA         -112
#define   BAD_Z_VALUE          -113  /* bad calc from focus function */
#define   BAD_STEP_PARAM       -114  /* slit step move in miscio.c   */
#define   BAD_SEM_INIT         -115  /* AllocSem failed              */
#define   SCSI_INITIALISE_ERROR     -200
#define   SCSI_INITIATOR_ERROR      -201
#define   SCSI_DEFINE_MODE_ERROR    -202
#define   SCSI_REQUEST_SENSE_ERROR  -203
#define   DISK_READ_ERROR           -210
#define   DISK_WRITE_ERROR          -211
#define   TAPE_UNIT_NOT_READY       -220
#define   TAPE_READ_ERROR           -221
#define   TAPE_WRITE_ERROR          -222
#define   TAPE_LOCATE_ERROR         -223
#define   TAPE_LOAD_ERROR           -224
#define   TAPE_UNLOAD_ERROR         -225
#define   TAPE_REWIND_ERROR         -226
#define   TAPE_MODE_SELECT_ERROR    -227
#define   BAD_PARAM_1     -501
#define   BAD_PARAM_2     -502
#define   BAD_PARAM_3     -503
#define   BAD_PARAM_4     -504
#define   BAD_PARAM_5     -505
#define   BAD_PARAM_6     -506
#define   BAD_PARAM_7     -507
#define   BAD_PARAM_8     -508
#define   BAD_PARAM_9     -509

/*
 *  Leitz table error replies.
 */
```

```
#define   NOS_L_ERRORS        3
#define   L_EXE00          -600
#define   L_OUTOL          -601
#define   L_BUE17          -602
#define   L_ERR00          -610   /* unknown Leitz error */
#define   SCSI_ERROR_FLAG    10000
#define   ASYNC_ERROR_FLAG   20000
```

Chapter 3

Setting up and testing the ADC/CCD

Accurate detection of relative light levels by the charge–coupled device (CCD) and accurate digitisation from the analogue-to-digital converter (ADC) plus associated electronics are of prime importance for data quality. The ADC printed circuit board has a number of offset and gain adjustments available which must be set up correctly to ensure optimum machine performance in terms of linearity and dynamic range. When new circuitry is added, the CCD and/or reference photodiode are changed or when changing the electronic offsets and/or gains in the system, checks should always be made to ensure accurate measurement of light levels for good astrometry and photometry from photographic plates. This Chapter described the set–ups and checks that should be performed in the event of any maintenance to the CCD/ADC scanning system.

3.1 Adjustments on the camera printed circuit boards

3.1.1 Setting up the ADC

The integrated circuit package containing the ADC and sample/hold systems has offset and range inputs that must be adjusted for each individual device installed. The full procedure for setting up such high specification ADCs is beyond the scope of this manual; however it is worth mentioning at this point that checks should be made with an accurate digital analyser that the offset and range are set correctly for the system. The procedure is iterative, since setting the offset and subsequently adjusting the ranging usually perturbs the original offset setting. In outline, the procedure is: adjust the offset so that for a 0V reference input only the least significant bit output from the ADC is toggling high/low; then the range should be adjusted so that all bits are set for a 10 V reference input. Further small adjustments to both should then be made to ensure that both are set correctly; in addition it is advisable to check that for 5 V the ADC outputs a mid–range value (*i.e.* 32768 for 16–bit digitisation). Note that the data acquisition transputers in the SuperCOSMOS system discard the least significant bit output by the ADC to avoid signed 2–byte integer overflow in the pixel processing software; hence it is not possible to examine the least significant bit output from the ADC by taking data with the system. Note also that VR8 and VR9 are the pots for the offset/range adjustment.

3.1.2 Setting the bias levels

As is the case in all CCD/ADC digitisation systems, electronic offsets are applied at the pre–amplifier stages between the CCD and ADC in order to prevent noise from making the ADC input drop below the lower voltage limit for digitisation. The SuperCOSMOS ADC is set to digitise between 0 V and +10 V, hence small positive DC offsets are applied in the pre–amplifiers for the reference channel, 'channel A' (even CCD pixels) and 'channel B' (odd CCD pixels).

For the CCD data channels, preset potentiometers VR 6 (channel A) and VR 5 (channel B) should be adjusted to set the time–independent component of the bias to ~ 200 ADU. For the reference channel, a preset potentiometer on the reference photodiode board is adjusted to offset those data. Note that because in the reference channel the time–dependent component of bias (*i.e.* the dark current – see Section 4.2.1) is relatively large, ~ 0 ADU time–independent offset is acceptable in the reference channel. Section 4.2.4 gives the procedure for measuring the dark components.

3.1.3 Bias level: checking the accuracy of digitisation

The original ADC camera boards installed on SuperCOSMOS were found to exhibit 'sticky bits', *i.e.* the few least significant bits output from the ADC showed $> 90\%$ probability of being constantly set or constantly clear (obviously, the presence of noise should mean that these bits toggle at random, with equal probability of being at 1 or 0). The reason for this was never determined to any degree of satisfaction; however it is suspected that the older ADC integrated circuits were malfunctioning due to operating at the extremes of their specification. Moreover it was found that, by setting the bias level up to ~ 10000 ADU, those ADCs could be made to digitise accurately. As a matter of caution, new ADC circuitry should be checked for stuck bits, but it is not expected that any problems will be found (*i.e.* it should not be necessary to increase the bias levels). To check for accurate digitisation, use the command `bitmap` (see Section 2.10.4) on data taken at all light levels.

3.1.4 Setting the gain levels

In order to maximise the dynamic range of the system the gain of the CCD data channel pre–amplifiers should be adjusted so that the point at which CCD saturation just occurs is close to the maximum digitised output value (*i.e.* 32767), provided that no electronic systems are disturbed by the large voltages produced under heavy saturation (see the next Section).

The gains are changed by adjusting preset potentiometers VR 1 (channel A) and VR 2 (channel B). Using the filter 1.0ND in the test chart (see Section 5.2.1) the table should be positioned and the light source set so that data close to saturation and just into saturation can be taken:

```
cosaxp0> absmov xy- 185. 170. 395.
cosaxp0> movewheel 8 0 20
cosaxp0> shortdarktime unsat.dat
cosaxp0> movewheel 7 0 20
cosaxp0> shortdarktime sat.dat
```

The gains should be adjusted so that when the CCD is just saturated, the ADC input voltage is just under 10 V. Then, the unsaturated data should have peak CCD counts at ~ 25000 ADU.

3.1.5 Gain level: checking the saturation response

When the CCD is over–illuminated, the output voltage reaches a limiting value, and the CCD is saturated. The peak output voltage from the CCD module is about -1 V (the CCD module output is negative). This signal is amplified and inverted on the camera board so that the signal lies in the range 0 to 10 V when it is supplied to the ADC. As stated in the previous Section, the amount of gain in that amplification stage is adjustable, and should be varied so that the full dynamic range of the CCD is used.

In practice, it is found that the output voltage from the CCD module continues to increase slightly beyond the nominal -1 V when the CCD itself has saturated, up to a maximum value of about -1.2 V, when it is heavily saturated. It is important that the ADC and associated circuitry can cope with any voltage produced under heavy saturation, since when scanning a dark plate with the highest light level available occasional emulsion flaws or scratches result in small transparent regions that will flood the CCD pixels with light.

The effect of too high a gain setting could be observed by scanning the darkest filter in the test chart (ND2.0) with the filter wheel set to clear air. Load the test chart (see Section 5.2.1), then:

```
cosaxp0> absmov xy- 384. 341. 395.
cosaxp0> movewheel 16 0 20
cosaxp0> locate 500 image.dat
cosaxp0> displaysc image.dat
...
```

Over most of the filter the CCD output is not saturated, but the occasional pinhole or scratch is present which causes the CCD locally to enter heavy saturation. If the ADC or integrating pre–amps fail to recover *immediately* after having being supplied with an out–of–range voltage, then horizontal bands will be seen in the data originating at the transparent feature. This effect would also occur on a photographic plate, and hence the gains would need to be reduced until such effects just disappeared. The original ADC circuitry for SuperCOSMOS was so sensitive to voltages above 10 V that the gains had to be set so that the CCD output was never amplified above that level. This limited the dynamic range of the system. The new camera electronics, incorporating an Analogic ADC, seem to be much more robust, and the gains have been set high in order to maximise dynamic range. Checks with the ND2.3 filter show saturated pinholes but also that accurate digitisation resumes as soon as the light level falls below the CCD saturation point. Furthermore, examination of the integrating pre–amp outputs with an oscilloscope also shows them to be reset from saturation so that unsaturated data are unaffected by previously saturated signals.

3.2 Testing the linearity

Implementation note: currently, no non–linearity adjustment is set–up in the SuperCOSMOS system. Measurements (see the subsequetn Sections) show that the maximum departure from linearity between the reference and CCD channels is $\sim \pm 5\%$.

3.2.1 Linearity requirements

Although any non–linear response is irrelevant to the system calibration as a whole, since the photographic process is non–linear anyway (intensity levels should be corrected by the transmission–to–intensity calibration measured from the step wedge spots available on each plate measured), it is nonetheless necessary to correct any differential non–linear response to small fluctuations in light level between the CCD and reference channels in order for the reference correction to work accurately. The problem with deriving the non–linear component in the response is that no 'gold standard' linear signal exists in the system. However, we can derive empirical corrections by obtaining data with linear correction LUTs in place and then examining the relative responses, to small fluctuations in light level, in the CCD and reference data for different CCD signal levels. Moreover, it does not matter where the non–linearities are occuring in the system (*e.g.* in the CCD and/or reference channels; in the silicon substrate of the reference photodiode and/or CCD pixels; in the analogue electronics). The only assumption that we make is that any CCD non–linearity is the same for all pixels, and is constant with time.

Global non–linearity measurements were made using the old illumination system and methods detailed in the old documentation by Lance Miller. The data derived can be found in files `/sdata/scos/machine/oldboard.*.linearity`. That procedure is no longer possible using the current system, however two scripts are provided to check the linearity of response (`checklinearity`) and measure the non–linearity from scratch (`measurelinearity`) to examine how the machine performs and indicate if any changes are necessary to machine parameter files.

3.2.2 Measuring the linearity

The following procedure should be carried out when any change is made to the camera electronics and/or when the CCD is changed. The approach adopted is to measure the response of the CCD to small fluctuations in light level relative to those in the reference channel. Under normal operating conditions, a linear LUT is loaded for the reference channel, and the CCD response is altered via a derived non–linearity LUT.

First, load the test plate containing the three ND filters into the machine (Section 5.2.1). After following the set–up procedure detailed in Section 2.4, run the script `measurelinearity`. This script uses combinations of filter wheel ND along with that available in the test chart to take data with linear LUTs loaded and all scan–time corrections disabled. Within the data files obtained, both the CCD and reference channels will show fluctuations in intensity due to variations in table speed. If the system is behaving linearly, at all CCD count levels a plot of fractional fluctuation in CCD level against fractional fluctuation in reference level should have unit slope, after the appropriate bias values have been subtracted (these are applied to the raw data using program `datacorrect`). Program `correctref` provides such plots – see Figure 3.1. The slope of the graph, calculated via a linear least–squares fit, is measured at 32 different CCD count levels ranging from ~ 100 ADU to $\sim 22,000$ ADU. The values of the slopes versus CCD count levels should then be extracted, sorted and 'arrowed' into a file and that filename given to the program `mknonlinlut` as in the following example:

```
cosaxp0> cd /disk1/scos
cosaxp0> rm data* gks*
cosaxp0> measurelinearity 500 > linearity.log
cosaxp0> grep Results linearity.log | sort +1 -3 > results.dat
cosaxp0> mknonlinlut
Input file containing slopes data:
results.dat
Output file to contain non-linear LUT:
newccd.linearity
```

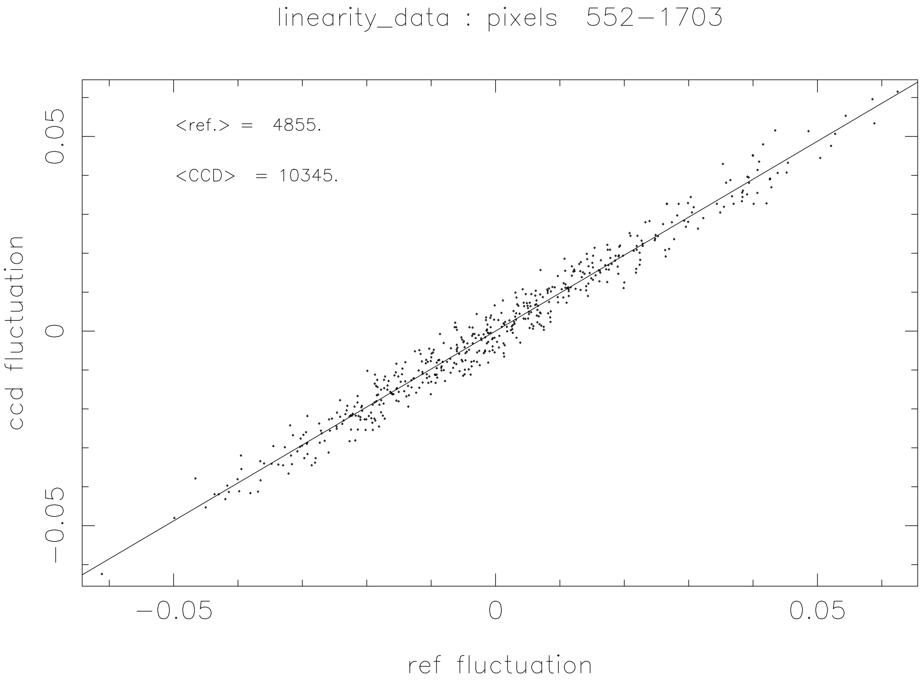

Figure 3.1: Displayed output from **correctref**. Fluctuations in light level in CCD data plotted against those in the reference channel should have unit slope if the reference corrections are to work accurately.

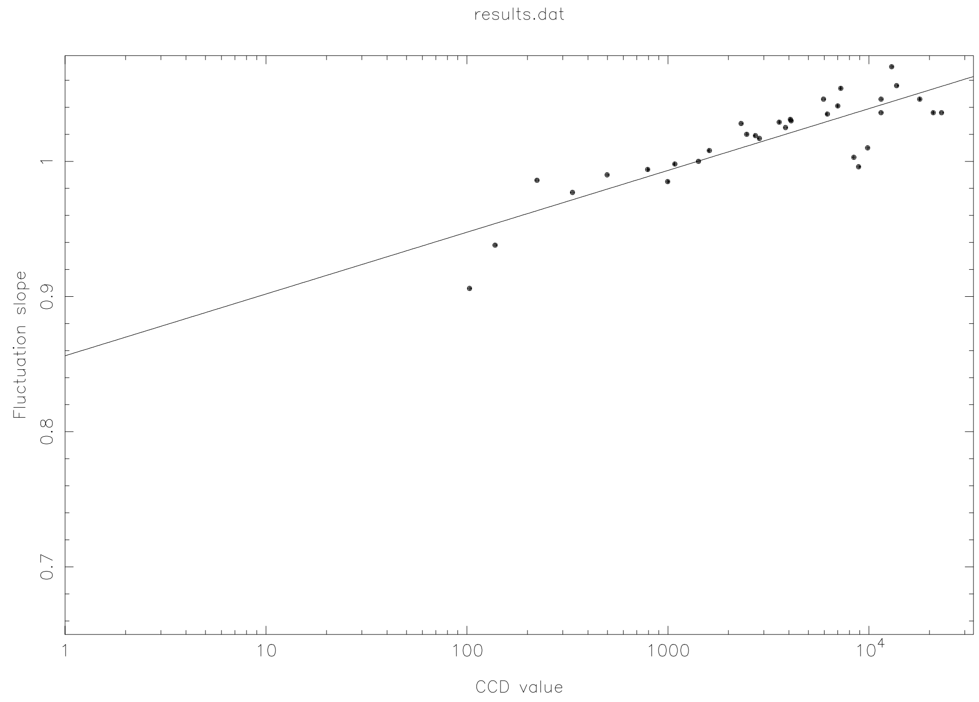

Figure 3.2: Displayed output from **mknonlinlut**. The slope of fluctuations in light level in CCD data against those in the reference channel plotted as a function of CCD value.

```
Mean bias level to offset LUT by (eg 340 ADU):
340.0
 Graphics device/type (?  to see list, default xwindows):
xwindows
Order of polynomial fit to fluctuation gradients:
2
mknonlinlut info: LUT does not reach 32767:
Maximum value =    30256.30
```

This program creates an appropriate non–linear LUT for the CCD; see Figure 3.2 for typical data. The file should be copied into the machine directory (having first renamed the old file), and then checked using script `checklinearity`:

```
cosaxp0> cd /sdata/scos/machine
cosaxp0> mv ccd.linearity ccd.linearity.old
cosaxp0> cp /disk1/scos/newccd.linearity ccd.linearity
cosaxp0> getdark
cosaxp0> cd /disk1/scos
cosaxp0> mkdir measured
cosaxp0> mv gks* measured/.
cosaxp0> mv data* measured/.
cosaxp0> checklinearity 500 > checklinearity.log
```

This script is identical to `measurelinearity`, except that it loads in the run–time linearity LUTs `ref.linearity` for the reference channel (which is in fact just a copy of the linear

`linear.linearity`) and `ccd.linearity` for the CCD data. Note that it is necessary to issue a new `getdark` command once a new CCD linearity file has been derived (NB: see Section 4.2.4 for the correct procedure to derive a darkframe). This time, the slope of the line should ideally be unity at all CCD count levels. Any non–unit slope which is output from `checklinearity` is needed for input as the final parameter for the transputer reference calculations (*e.g.* the input parameter to `CALC_2` in the shell scripts). As a facility exists only to input a single value for that slope, it should be chosen as representative of the CCD levels that will be encountered when scanning photographic data. The higher level software also has this number 'hard–wired' — the value should be changed, if found necessary, for optimum machine performance. The current value for this number is 1.0, *i.e.* the calculation does nothing since the non–linearity LUT `/sdata/scos/machine/ccd.linearity` accounts for all the necessary non–linear response.

3.3 Testing the CCD for charge trapping

Section 3.2 describes how to test the response of the CCD to small fluctuations in light level, against those in the reference channel, at all light levels. If, at any level, the CCD response suddenly drops to zero then it is likely that the CCD is suffering from bulk charge trapping. For example, it was found that the first CCD installed on SuperCOSMOS exhibited bulk charge trapping at about one–third full–well, in which the CCD stopped responding to small fluctuations in the amount of light received (over the range from ~ 9000 ADU to $\sim 11,000$ ADU). This effect was discovered using the procedure detailed in Section 3.2. Obviously, any device exhibiting such behaviour is unusable and must be discarded.

3.4 Measuring the system dark noise

The system noise in the absence of light can be measured by obtaining a scan of data with all corrections applied and the CCD light path blocked. Program `mean` can then be used to measure the RMS fluctuations of each pixel. Typical noise values should be ~ 3 ADU per pixel.

To measure the system noise, use the following command sequence:

```
cosaxp0> movewheel 0 0 20
cosaxp0> absmov xyz 200. 200. 395.
cosaxp0> locate 100 noise.dat
cosaxp0> pixelplot noise.dat
...
cosaxp0> mean noise.dat
...
```

Chapter 4

Scan corrections

Scan corrections are applied in real–time by the transputers to the raw CCD data. There are four corrections, which are applied in the following order:

1. Non–linearity correction
2. Bias subtraction
3. Flatfield correction
4. Reference correction

The real–time corrections themselves are implemented in C code written by Jim Herd. The implementation of the corrections may be tested using engineering data as described previously in Chapter 2.

4.1 Non–linearity correction

Both the CCD and the reference channel are expected to show a non–linear dependence between the input illumination level and the output signal level. Initially, it might be thought that correcting for this effect is unnecessary because the photographic response itself is already non–linear (*e.g.* see Section 3.2). However, if either the CCD or reference channel outputs are non–linear, the subsequent real–time corrections described in this Chapter would not work correctly.

Correction for non–linearity is applied by means of a look–up table (LUT) between the incoming data value from the photoelectric device (CCD or reference channel photodiode) and a linearised output value which is passed on to the next step in the processing chain. Input data values are two–byte numbers; output values are four–byte floating point numbers. Hence, this stage of the processing also does the conversion from integer to real numbers which is required for the subsequent floating–point operations in the real–time correction software.

Every CCD value is corrected by the same non–linearity LUT, *i.e.* it is assumed that each pixel exhibits the same non–linearity. At the saturation level this assumption becomes invalid, but otherwise appears justified (the reference channel has a separate LUT). Furthermore, a facility is provided to apply a two–stage non–linearity correction. Section 3.2 provides further details, describes how to check the existing non–linearity corrections, and describes how to derive new ones. Chapter 2 provides further information on the data file format for the LUTs, and how to load them into transputer memory on startup.

4.2 Bias subtraction

The CCD and reference channel return non–zero output counts when not illuminated. In order for the flatfield and reference corrections to work accurately, these 'dark' values need to be subtracted. In practice, there are two contributions to the dark values which need to be treated separately.

4.2.1 Dark signal dependent on integration time

As in every solid–state photoelectric device, electron/hole pairs are generated thermally within the substrate, which results in a non–zero signal being output even when the device is not illuminated. In SuperCOSMOS, the CCD is operated at a temperature of $20.0 \pm 0.1°$ C and has an 8ms integration time. That generates a signal which when digitised amounts to about 20 ADU. The dark current itself also suffers from shot noise, but the noise on that signal is insignificant compared with other noise sources in the system. The reference photodiode and associated electronics (used for the final real–time correction described in Section 4.4) also suffer from dark current. The value of the dark signal there is higher, about 90 ADU.

These components of dark current have linear dependencies on integration time. When the system is scanning, the integration time between readouts varies, causing variations in both the received amount of light and in the amount of dark current. Fluctuations in the data due to variation in integration time are removed by the reference channel correction (Section 4.4), and because the components of dark current described here also depend on integration time, they must **not** be subtracted from the data values before applying the reference correction. While *variations* in count levels due to variation in integration time are removed by the reference correction (see Section 4.4), the zero–point time–dependent dark component is not subracted from the data, which results in a dark signal (commonly known as $T_{\rm black}$) of about 20 ADU in the final CCD data. To examine the $T_{\rm black}$ values type the following:

```
cosaxp0> cd /sdata/scos/machine
cosaxp0> flatfieldplot black 7 15 xwindows  # for ref channel black values
cosaxp0> flatfieldplot black 43 2090 xwin   # for the 2048 CCD black values
```

4.2.2 Dark signal not dependent on integration time

In addition to the time–dependent dark signal described in Section 4.2.1, there are two contributions to the dark signal which do not vary with integration time. The first of these is dark current generated elsewhere in the system. The most significant contribution is made in the CCD shift registers, which generate around 4 ms of dark current regardless of the time between readouts. The second is introduced by electronic offsets within the system (see Section 3.1.2). These offsets are adjusted to give bias values at the level of ~ 200 ADU.

Both corrections can be evaluated by extrapolating the output of the CCD and reference channels to zero integration time. These corrections vary significantly between odd and even CCD pixels as they have two independent pre–amplifier channels on the camera board and the electronic offsets in those channels will never be set precisely the same. Hence, every pixel has it's own bias value. A file of these values (`/sdata/scos/machine/dark`) is loaded into the transputers and the bias values are subtracted from every pixel as they are processed through the scan corrections chain.

Time variations in the bias frame

In order to achieve accurate results the bias values need to be subtracted to an accuracy of order 0.1%. If the DC offset voltages are set to give a high bias value (say of order 10000 ADU), fluctuations in that voltage with time will cause variations in the bias value of about 20 ADU; thus it is necessary to remove these time fluctuations. If the bias value is only a few hundred ADU, there is no need for the resulting small fluctuations to be removed.

The scan–time correction software is set to calculate fluctuations in the bias. The method is to monitor a set of dark pixels in the readout. When data are being collected, at each scan the values of pixels 34 to 41 (inclusive), defined with the first pixel being zero, are averaged to provide a monitoring value. One point of detail is that these values should average to zero over time: this is achieved by subtracting the bias frame values from these dark pixels before the fluctuation is calculated. Note, however, that since the bias levels are set low in the current system (and hence any fluctuations in those bias levels are expected to be insignificant) the fluctuation is not subtracted from the data — such a correction would only add noise into the final data (albeit at a low level).

4.2.3 Calculation of the bias frame

A constant frame of bias values must be subtracted from every scan. That bias frame should contain, for each pixel, the value of the bias which is independent of integration time only. The bias frame is calculated using a scheme which can eliminate the time–dependent component. The approach adopted is to measure the total dark signal when the table is scanning at two different speeds (usually 1.0 mm/s and 1.6 mm/s). For each pixel, a linear fit is made to the measured value as a function of integration time: extrapolating to zero integration time gives the time–independent bias value for each pixel. A complicating factor is that during such measurements of the dark signal, the electronic offsets may also be fluctuating (see above). If large and ignored, such fluctuations would completely swamp the variations in measured values due to the change in integration time. There is no easy solution to this. The approach adopted is to make four dark measurements, with speeds 1.0, 1.6, 1.6 and 1.0 mm/s in that order. Data for the two speeds are averaged, so that a linear variation in electronic offset with time will be removed. Note that this is not expected to be a problem in the present system since the bias level offset voltages are set low and fluctuations on those voltages will be very small.

4.2.4 Procedure for measuring the bias frame

To measure a new bias frame, first set up the system as described in Chapter 2. Then, to cut off all light through the system type:

```
cosaxp0> movewheel 0 0 20
```

and close the shutter on the Xenon lamp housing (silver knob at the top back of the unit). This is necessary to cut off the light in the reference channel — in fact, to totally extinguish any light in the reference channel it would be necessary to remove the lid on the collimating optics and lift the 45° reference sample glass to vertical, otherwise errors of a few ADU and higher noise result in the reference channel dark values. However, it has been decided that these errors are insignificant and that to minimise the risk of damage to the reference sample mirror, it should not be disturbed. When the system is set up and the light paths blocked (note also that the chamber and control room lights must be off and all the blinds on the chamber windows lowered) execute the bias script as follows:

```
cosaxp0> getdark
```

New dark and black frames will be derived; the dark values will be loaded into the transputers. The files are written to the machine directory **/sdata/scos/machine**, and old files renamed to the current time and date. Once the task is finished, be sure to restore the light paths by reopening the shutter on the lamp housing. The dark and black frames may then be inspected:

```
cosaxp0> cd /sdata/scos/machine
cosaxp0> flatfieldplot black 6 16 xwin
cosaxp0> flatfieldplot dark  6 16 xwin
cosaxp0> flatfieldplot black 43 2090 xwin
cosaxp0> flatfieldplot dark  43 2090 xwin
```

4.3 Flatfield correction

4.3.1 The application of the flatfield

The response of the combined optical system and CCD varies from pixel to pixel due to variations in illumination through the optics and due to variations in quantum efficiency and physical area of each pixel on the CCD. These variations may be corrected for by dividing the bias–subtracted data by a flatfield frame.

The flatfield frame is stored as a file of real numbers, one for each pixel, which is generated prior to each plate measurement. The values are loaded into the transputers for real–time scan correction (Section 2.4.6). Subtle variations in the flatfield shape are caused by different refracting/reflecting surfaces in the optical path; this necessitates generating a flatfield frame at the actual filter wheel setting which is used for the plate measurement, with the plate in place.

In the CCD portion of the data the values of the flatfield are around unity, so that when the data are divided by the flatfield, the output values are similar in magnitude to the input values. This ensures that the full dynamic range of the measurement is preserved, without any danger of the output values exceeding the allowed dynamic range. It also ensures that it is possible to check that the light level was not so high that the CCD was saturated.

In the reference portion of the flatfield file, the values for each reference pixel correspond to the actual expected value for that filter wheel setting, *i.e.* the flatfield reference values are not normalised to unity. In that way, the ratio of an actual reference data value obtained during a scan to the expected number from the flatfield comes out close to unity, and that ratio can then be used in the reference correction as described in Section 4.4. On output, if flatfielding is turned on as in normal use, the reference values which have been divided by their flatfield values are multiplied by a factor of 10000 so that small fluctuations in reference level may be investigated if necessary, without losing that information because of conversion back to integer values on output.

4.3.2 Flatfield accuracy

The accuracy of the flatfield is vital to the successful detection of faint objects and to the correct matching of data across scanning lanes. Because the same flatfield is applied to every scan, random noise in the flatfield appears as a systematic error in the data from a plate measurement. Flatfield errors show up as vertical stripes in the data, and possibly as a discontinuity in background brightness at lane boundaries. On SuperCOSMOS, the flatfield needs to be accurate to at least 0.3%.

4.3.3 Flatfield types

There are two different methods of generating flatfields: we refer to these as the *median method* and the *matrix method*. Each method has advantages and disadvantages, and the best method to choose depends on the nature of the measurement being undertaken. In general, however, the matrix method is to be preferred for routine plate measurement.

The median method

In this method a number of scans (usually 3000) are taken of either clear air or through a neutral density filter which is known to be reasonably clean and free from scratches. For each pixel, the median is evaluated to both improve the signal-to-noise over a single measurement and to eliminate occasional extreme pixel values, especially those due to dirt or flaws on the neutral density filter. In the CCD portion of the data, the values are all normalised by the value of the highest pixel, so that output values in the range 0.9 to 1.0 are typically produced.

The method has the advantage of extremely low random noise, typically about 0.01%, but it does have the following disadvantages:

1. The plate needs to be removed in order to obtain the flatfield.
2. For the highest ND settings, the flatfield measurement can be made through clear air, but for lower ND settings additional ND must be inserted using the test plate and the data collected from the correct location.
3. Because the data are not being collected with the plate in position, the glass thickness which is used in the flatfield determination (either zero or the thickness of an ND filter) differs from that used in the plate measurement. This may change the flatfield shape due to optical effects and errors in slit alignment at different slit positions, and consequently introduces the possibility of systematic errors into the process.

The matrix method

The second method allows a flatfield to be derived with the plate in position. By analysing data taken at a series of positions which are offset along the axis of the CCD, it is possible to solve for the flatfield distribution in a way which is independent of the transmission values through the plate. Further details of the method are given in Section 4.5. The method has a number of advantages:

1. The plate does not need to be removed in order to derive the flatfield. This results in less plate handling and potentially quicker turnaround. It then becomes feasible to derive a flatfield for each plate measurement individually, and the resulting flatfield will thus be more immune to time variations in the flatfield.
2. The flatfield is then guaranteed to be derived correctly for the plate being measured, provided no system parameters are changed in the time between deriving the flatfield and scanning the plate. In particular, errors in the illumination slit position will not affect the flatfielding accuracy.

There are disadvantages, however:

1. The current data collection and processing time when deriving the flatfield is rather long, about 15 minutes, which somewhat offsets the potential gains of the method. This can be improved by more efficient data collection in the transputers in future.

2. If the amount of data is restricted to that which can be currently collected and processed in 15 minutes, the signal-to-noise in the derived flatfield is about ten times worse than with the median method, *i.e.* about 0.1%. For most applications this amount of flatfield uncertainty is acceptable, but for low–noise applications, such as digital stacking of data or when searching for low surface–brightness objects, the median method may be preferred since random errors in the flat translate to systematics in 2d image data as every scan is divided by that same flatfield frame.

4.3.4 Derivation of flatfield frames

After system set–up as described in Chapter 2, the procedures are as follows. The median method of obtaining the flatfield may be actioned by executing the command:

```
cosaxp0> getflatfield <n>
```

where `<n>` is the ND filter wheel setting required. The matrix method may be actioned by typing the command:

```
cosaxp0> getplateflatfield <plate type> <n>
```

where `<n>` is as before, and `<plate type>` is either `copy`, `original` or `noslit`. The latter leaves the slit in its current location, saving time if the operator is confident that the slit does not need to be repositioned, or if some non–standard slit setting is needed, *e.g.*:

```
cosaxp0> slitmov 2.0 100              # position slit for a 2mm plate
cosaxp0> getplateflatfield noslit 10 # get flatfield at filter wheel step 10
cosaxp0> cd /sdata/scos/machine                # change to machine directory
cosaxp0> flatfieldplot flat10 552 1703 xwin   # display the results
```

4.4 Reference correction

The final real–time correction is for variations in light intensity and in table speed during a scan. In practice, it turns out that variations in table speed (up to 10%) dominate those in the light level ($\sim$ 0.1% RMS; $\sim$ 1% peak–to–peak). Because the CCD is read out every time the table has moved a fixed distance (10μm — see Section 1.4), the variations in table speed cause the integration time to vary between scans, and hence the amount of light collected varies. Such variations show up as horizontal stripes in image data.

Both these variations are monitored by means of a reference photodiode which is fed by a small diameter fibre–optic bundle from the illumination unit in the control room. The signal from the reference photodiode is integrated and sampled at the start of each readout, so that it closely follows variations in the CCD output. The reference signal is digitised by the same ADC as the CCD data, and appears as pixel values at the start of each raw scan. In fact, the reference signal is sampled many times, and these repeat measurements occupy pixels 1 to 16 in a raw scan. The first few of these values are affected by a time dependent offset in the data, so pixels 7 to 15 inclusive are averaged and used for the reference measurement. Thus, the fractional variation in the reference signal should provide the fractional correction which needs to be applied to each pixel. In order for the fractional correction to be accurately measured, it is necessary both for the non–linearity corrections to have been applied to both the CCD and reference channel data, and also for the bias values to have been subtracted. Note that because there are two components to the bias, time–dependent and time–independent, it is not possible with this system to precisely correct for both variations in light level and in table speed. However, as long as variations in table speed dominate, this problem is not important. Section 5.5 describes how to verify the stability of illumination.

By correlating variations in the reference signal with variations in the CCD data it is possible to verify that the reference correction is working accurately. In practice, it is found that the best linear fit to the CCD fluctuations as a function of fluctuation in reference value typically has non–unit slope. This is probably due to bias in the value of the slope due to noise in the reference channel. Since the reference channel suffers from noise during the application of the reference correction, it is probably best to allow the applied slope to have this non–unit value to help reduce the bias. The value of the slope is given to the correction software (*e.g.* the transputer program `CALC_2`) as one of its inputs. The derivation of the slope and further details can be found in Section 3.2.

4.4.1 'Out–of–range lamp values' error

Finally, the reference correction carried out by the `CALC_2` transputer also monitors the raw reference values against those obtained when deriving the flatfield for a particular plate scan — in fact, the monitor is set to examine the departure from unity of the normalised reference values when they have been divided by those in the flatfield frame. If the raw reference signal changes by more the $\pm 20\%$ from the flatfield value, this condition is flagged by the `CALC_2` transputer. Under normal plate scanning with the GUI, error messages are produced in the terminal window from which the GUI was launched:

```
cosaxp0>
***************************************************************

     999 out-of-range lamp values
     in lane number 9

***************************************************************
cosaxp0>
```

This was originally set up to advise the operator if the light level was fluctuating, but it also flags other problems in the system, *e.g.* digitisation problems, problems on the camera PCB. For example, if the on–board integration time changes by more than 20% from the drift speed readout of 8ms, this error would be reported; conversely if the drift speed of the table changes by more than $\pm 20\%$ from 1.25 mms^{-1} this error would again result. Note that the reference channel counts can change by up to $\sim 10\%$ when different ND is selected via the filter wheel. This is because different ND reflects different amounts of light back up th light path to the reference channel in the illumination unit. Hence, use of a flatfield frame other than that derived with the same ND as when measuring the plate (which would *not* be recommended for a number of reasons) may give rise to such error reports.

4.5 Matrix flatfield method and algebra

The aim of the matrix method is to enable a flatfield to be derived even when a photographic plate is present in the light path. This method should give reasonable results provided that no part of the light path is too dark.

The concept of the method is best illustrated by the following example. Let us denote the flatfield factor for each pixel i as f_i and the true transmission of the photographic plate (as measured by as system with uniform pixel response) as d_i. When we take a scan we measure each of the products $s_i = f_i d_i$. Suppose we take two scans through the photograph in which the CCD has been moved by exactly one pixel along its length. Then, the second scan will comprise measurements of the products $s'_i = f_i d_{i+1}$. Hence the ratio $s'_{i-1}/s_i = f_{i-1}/f_i$. The unknown photographic transmission values can be eliminated. Since the ratio of flatfield values can be measured in this way for all adjacent pixels, it is then possible to calculate the flatfield value of any pixel with respect to, say, the first pixel in a scan. Since the flatfield frame is normalised to values about unity in any case, the absolute quantum efficiencies of the pixels are not required: the relative values are sufficient.

In practice, such a procedure would be very noise, because in order to calculate the flatfield value of, for example, pixel 2000 with respect to pixel 1 we need to multiply 1,999 measured ratios together. The technique can be greatly improved by measuring not only the flatfield ratios for adjacent pixels, but also the flatfield ratios of pixels over a range of offsets up to the maximum size of the CCD. There is then a least–squares solution to the entire set of measurements which allows the 'best' set of relative values to be calculated.

Suppose we take one such pair of measurements. We can write a matrix equation of the following form:

$$\begin{pmatrix} 1 & 0 & -1 & 0 & 0 & 0 \\ 0 & 1 & 0 & -1 & 0 & 0 \\ 0 & 0 & 1 & 0 & -1 & 0 \\ 0 & 0 & 0 & 1 & 0 & -1 \end{pmatrix} \begin{pmatrix} \log f_1 \\ \log f_2 \\ \log f_3 \\ \log f_4 \\ \log f_5 \\ \log f_6 \end{pmatrix} = \begin{pmatrix} \log(s'_1/s_3) \\ \log(s'_2/s_4) \\ \log(s'_3/s_5) \\ \log(s'_4/s_6) \end{pmatrix}.$$

The LHS can be written $\sum_i a_{ik} \log f_i$. If we have estimates $\log \hat{f}_i$ for the values of $\log f_i$ then we can calculate estimates $\hat{x}_k = \sum_i a_{ik} \log \hat{f}_i$, and we want to minimise the least squares quantity

$$\begin{aligned} S^2 &= \sum_k w_k (\hat{x}_k - x_k)^2 \\ &= \sum_k w_k (\sum_i a_{ik} \log \hat{f}_i - x_k)^2 \end{aligned}$$

over all datasets, where we have allowed a set of weights w_k in order to influence the relative merits of measuring relative flatfield values over large or small offsets. The current implementation of this algorithm has all weights set to unity.

By differentiating with respect to each of the values $\log \hat{f}_i$, we find:

$$\begin{aligned} \frac{\partial}{\partial \log \hat{f}_i}(S^2) &= 2 \sum_k w_k (\sum_i a_{ik} \log \hat{f}_i - x_k) a_{jk} \\ &= 0 \end{aligned}$$

when

$$\sum_k w_k a_{jk} \sum_i a_{ik} \log \hat{f}_i \quad = \quad \sum_k w_k a_{jk} x_k$$

or

$$\sum_i \log \hat{f}_i \sum_k w_k a_{jk} a_{ik} \quad = \quad \sum_k w_k a_{jk} x_k.$$

If the CCD has n pixels, then the LHS square matrix is of size $n \times n$. It is symmetric, and for many fewer offsets than pixels, it will be only sparsely filled. The above equation is not immediately soluble, however, as the LHS is always singular. This is because there is no unique solution: the measurements can only provide us with relative flatfield values, whereas the above equation gives us estimates for all flatfield values. To solve the equation we set one (arbitrary) pixel flatfield value to unity. This results in the deletion of one column of the LHS matrix. If we discard the corresponding row, then the matrix remains square and symmetric and a unique least–squares solution can now be found (the loss of information caused by the deletion of the row will have a minimal effect on the accuracy of the solution). Provided large offsets as well as small offsets are included in the measurement, then the matrix equation can be solved using the NAG routine `F04MBF`, as in the program `matrixflat.for`.

It was mentioned above that the method will give poor results if some portion of the photographic plate is unusually dark. The method will also perform poorly if the photographic transmission of any one portion varies between measurements, for example because of dust moving on the plate. We might also expect poor performance in regions where there are large gradients in photographic density, because then small positioning errors will result in erroneous flatfield ratios being derived. To help guard against all of these, the implementation of the algorithm on SuperCOSMOS carries out nine such measurements at different Leitz x–axis positions, median filtering the results from each of these sets of measurements. The implementation also averages many scans at each CCD location in order to eliminate photon shot noise from the measurements. The offset values, the number of integrations per position and the number of x–axis sets are all hard–wired into the the program `matrixflat` and hence if these are altered then `matrixflat` needs to be altered accordingly and recompiled.

One final practical point to note is that the matrix size is independent of the amount of data taken – it depends only on the size of the CCD. As the solution time on a Sun SPARCstation is typically 10 minutes, most efficient usage is obtained by spending at least that amount of time collecting data.

Chapter 5

Imaging system set–up

The imaging system consists of the illumination unit, slit projector unit, and CCD camera. It is unlikely that any adjustments or modifications to the telecentric lenses will be needed in the future — no set–up information will be given here for these lenses. Procedures are described, though, for testing the optical performance of the imaging system. However it is possible that a new CCD will be required at some point in the future. This Chapter also describes how to change the lamp in the illumination unit.

In order to achieve accurate registration of lanes, and in order to reduce systematic errors in position to a minimum, the CCD camera needs to be accurately aligned and positioned. If the CCD camera is removed from SuperCOSMOS, then all alignments should be rechecked on replacement. If the bridge is disturbed for any reason (this could result from accidental collision, work on the slit projection unit, or removal of the Leitz machine covers for maintenance work) then the bridge rotation will need to be checked and adjusted as necessary. Regular checks of bridge rotation should be made, but the other CCD camera alignments should be stable if the camera is left undisturbed.

Obviously, the slit must be accurately aligned with the CCD camera in order for the full length of the device to be illuminated. Moreover, for optimum throughput in the system, the slit needs to be accurately focussed for each plate type measured. If the slit is not aligned and/or the focus position has moved for some reason (*e.g.* maintenance work on the slit projector unit) then it should be realigned and focus redetermined.

The following Sections give prescriptions for measuring all the necessary CCD/slit alignments using engineering software routines for driving the machine, for collecting the data and for analysing it. Source code, executables and shell scripts are held in the directories described in Section 2.2.1. Some of the tests described below rely on accurate measurement of a test edge. This is provided by the black edges available on the photographic MTF chart held in the SuperCOSMOS test plate (this plate has four locations: one for the MTF chart, the others for neutral density filters having ND values ~ 0.5, ~ 1.0 and ~ 2.0). Before any of the tests can be carried out, the system must be set up to operate in engineering mode (Section 2.4).

5.1 Starting up

To set the system up, the following commands need to be issued (see Section 2.4 for a complete description):

```
cosaxp0> source ~scosdev/v033/.login   # set up system paths and software
```

```
cosaxp0> setenv PATH {$PATH}:/home/scosdev/v033/lam/bin  # add in the paths
cosaxp0> setenv PATH {$PATH}:/home/nch/scos/scripts      # for other scripts
cosaxp0> setenv PATH {$PATH}:/disk1/nch/scratch/bin/osf  # and software
cosaxp0> loadsys              # set up the transputer system
cosaxp0> autozero             # reset and datum the table
cosaxp0> setparam 25 0 191    # disable Leitz table geometry correction
cosaxp0> getdark              # derive a new dark frame if necessary
cosaxp0> movewheel 1 0 20     # set the light level for clear air
```

Note that when a new dark frame is being derived it is very important to follow the procedure given in Section 4.2.4.

5.2 CCD Alignment

5.2.1 Positioning the MTF chart

Enter the SuperCOSMOS chamber and load the metal test chart into a plate holder, then load the plate holder into the machine in the usual manner. Throughout this manual, it is assumed that the MTF chart is oriented in the machine such that when facing the machine from the loading bay doors, the MTF chart is in the upper right of the four positions with the numbers on the chart reading correctly (*i.e.* **not** back–to–front due to the chart being in upside down). Positioning the table using the joystick (or `absmov` if outside the chamber) so that the readout (or result of `readpos`) is at $x = 200$ mm, $y = 339$ mm should then illuminate a suitable strip on the MTF chart for what follows. Note that some scripts (*e.g.* `getflatmtf`) will not work correctly if the test chart is oriented other than as suggested here.

5.2.2 Obtaining a flatfield frame

For precision measurements, a flatfield frame appropriate for the ND filter selected must be obtained through transparent parts of the MTF chart with the correct slit position. Script `getflatmtf` does this:

```
cosaxp0> cd /disk1/scos
cosaxp0> getflatmtf 1
cosaxp0> cp flat1 /sdata/scos/machine/flat
cosaxp0> loadcorrections flat
cosaxp0> absmov xyz 200. 339. 395.
```

The slit, filter wheel and table will now be in the correct positions and the appropriate dark and flat corrections loaded. The machine is now ready for the following alignment and other tests. Note that if a `loadsys` command is issued at any stage (perhaps because the system got hung up at some point) then the `loadcorrections` command should be reissued to reload the correction frames back into the transputers.

5.2.3 Manual focusing

Focusing at a particular position off the MTF chart can be achieved by running the shell script `takez` once the machine has been positioned at the desired location. Suitable features for

Figure 5.1: Displayed output from **takez** showing the flaring of MTF chart bars as the optical system goes out of focus.

focusing are dark bars perpendicular to the CCD – examine the oscilloscope trace in the control room to check that a number of such features are present along the length of the CCD. The routine `takez` steps the machine along its (vertical) z–axis in steps of 50 μm from Leitz z co-ordinate 393.0 mm to 396.95 mm. A single scan is taken at each z position, and an image file is created in the directory `/sdata/scos`. The image can be displayed using `displaysc`. The black bars of the test chart should be visible, with significant flaring for the scans which were out of focus – see Figure 5.1. The cursor option in `displaysc` should be used to select a small region containing a few narrow bars near the centre of the CCD (*i.e.* near the optical axis of the system); the pixel numbers to be used should be noted for input to the analysis program `focustest`. This requires the image file and the selected pixel range to be input. All input scan should be used (the default option). Under normal usage, for `xwindows` display the command `xdisplay` should be used. A plot will be produced showing two statistics: both measure the the statistic used by the normal SuperCOSMOS focusing routine, which is a measure of the pixel-to-pixel noise – see Figure 5.2. One plot shows the statistic for adjacent pixels; the other shows the same for alternate pixels. The best focus position can be read off the plots by noting the position of the maximum of one or both off these statistics. Note that the program assumes the data have been obtained with `takez` as described above: no information other than the raw data is passed to `focustest`. Hence, if the shell script `takez` is modified then the program `focustest` will also need to be modified and recompiled.

A typical command sequence for focusing might be as follows:

```
cosaxp0> takez focus.dat
...
cosaxp0> mv /sdata/scos/focus.dat .
cosaxp0> displaysc focus.dat
 scan length is      2090 : range of pixel numbers to use ? 552 1703
 number of scans is    80 : range of scan numbers to use ?    1   80
Plot device  [xwin] (? for help) xwindows
use left mouse button to read cursor value,
use right mouse button to exit
x =   844, y =    41, value =    14199
x =   916, y =    40, value =    13956
!! GRCURS - Error getting cursor position   # ignore this error message
x =   916, y =    40, value =    13956
cosaxp0> focustest focus.dat
 scan length is      2090 : range of pixel numbers to use ? 844 916
 number of scans is    80 : range of scan numbers to use ?    1  80
 Graphics device/type (?  to see list, default xwindows):
xwindows
cosaxp0> absmov --z 200. 200. 394.95
```

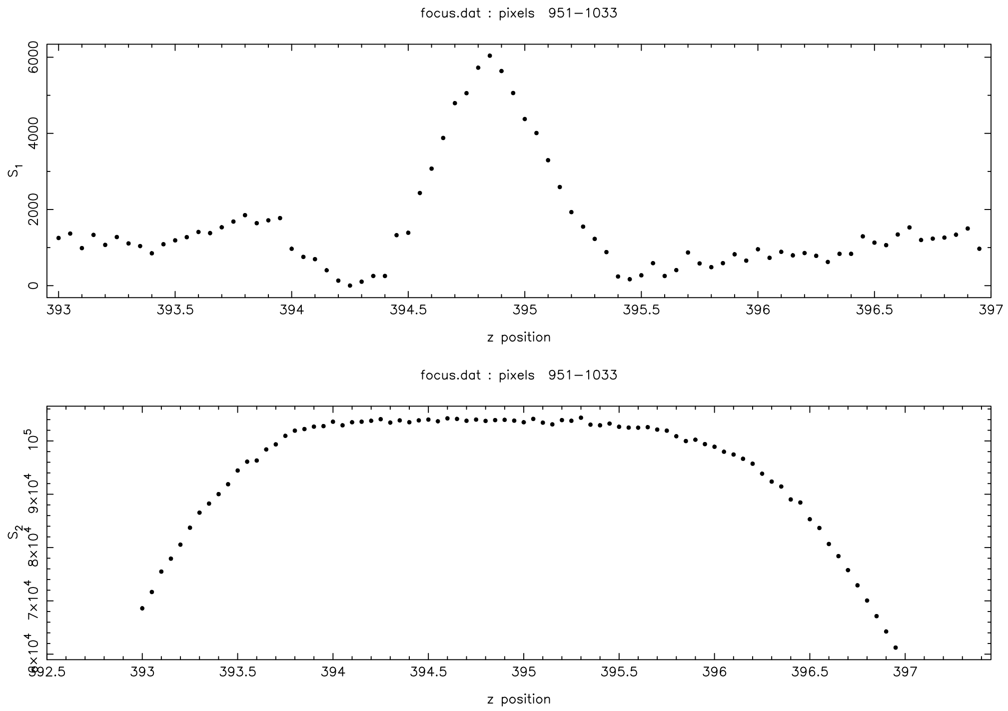

Figure 5.2: Displayed output from **focustest**. The best focus position is near the central value, at $z = 394.85$ (all the SuperCOSMOS plate holders are adjusted to have focus positions around $z = 395.0$ mm).

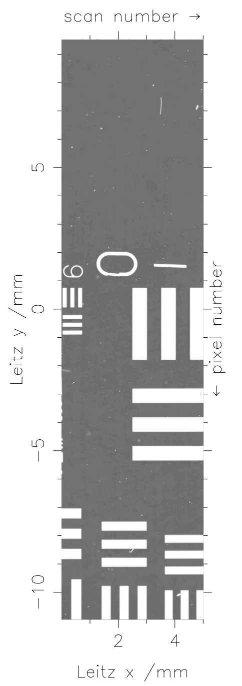

Figure 5.3: Displayed output from **lzdp**.

The final command moves the z–axis to the optimum focus position, at the same time leaving the xy position unchanged. The table is now ready to locate the required test edges for the alignment tests.

5.2.4 Location of test edges

Having focused on a region, the position of one edge needs to be accurately located. A vertical edge (*i.e.* perpendicular to the CCD) needs to be used for measuring the magnification error. A horizontal edge (*i.e.* parallel to the CCD) needs to be used for measuring the bridge rotation. It is assumed that the MTF chart is aligned so that it is not rotated with respect to the CCD – it is adequate to check the alignment visibly by scanning a small region and displaying it (great accuracy is not required for the alignment tests described below).

To locate an edge, the MTF chart should be scanned to obtain an image using the shell script `locate`. Note that `locate` does not return the table to the original position, and hence that position should be noted using `readpos` and if the scan needs to be repeated the table should be repositioned using `absmov`. This image can be displayed using the command `lzdp`, which produces a grey–scale plot with axes labelled in Leitz xy co-ordinates relative to the position at the start of the scan (see Figure 5.3). The cursor option can be used to find the approximate location of an edge; the output values are relative to the xy position at the start of the scan and correspond roughly to the position required to locate pixel 1000 at that part of the test chart. A more accurate determination of the position of the edge should then be obtained using shell script `xstep`, which steps the table in intervals of 10 μm in Leitz x, thus building up an image by discrete table movements rather than continuous scanning. The cursor option in `displaysc` should be used to measure the precise location of the edge (note that for output from `xstep` and `displaysc` the cursor position returned indicates the shift in units of pixels, *i.e.* 10μm from the start position given to `xstep`).

A typical command sequence might be as follows:

```
cosaxp0> readpos
X = 200.841170 :: Y = 333.998850 :: Z = 394.950000
cosaxp0> locate 500 locate.dat
cosaxp0> absmov xyz  200.841170 333.998850 394.950000
cosaxp0> lzdp locate.dat
 scan length is      2090 : range of pixel numbers to use ? 552 1703
 number of scans is   500 : range of scan numbers to use ?    1  500
 Graphics device/type (?  to see list, default xwindows):
xwindows
use left mouse button to read cursor value,
use right mouse button to exit
Leitz x =     1.7871, Leitz y =    -4.7489, value =     6203
!! GRCURS - Error getting cursor position   # ignore this error message
Leitz x =     1.7871, Leitz y =    -4.7489, value =     6203
cosaxp0> xstep 202 329.24995 394.950000 xstep.dat
                # NB: the start x position must be an integer, and the
                # output file has to be renamed to the working directory
cosaxp0> mv /sdata/scos/xstep.dat .
cosaxp0> displaysc xstep.dat
 scan length is      2090 : range of pixel numbers to use ?
 number of scans is   100 : range of scan numbers to use ?
Plot device  [xwin] (? for help) xwindows
use left mouse button to read cursor value,
use right mouse button to exit
...
```

5.2.5 Measurement of bridge rotation

If the CCD or the bridge have been moved, the principal axis of the CCD will almost certainly be misaligned with the Leitz y–axis. When scanning, this would result in a mismatch in pixel positions at the boundary between lanes and sawtooth positional errors perpendicular to the CCD. The rotational alignment can be measured by stepping each pixel in turn over an edge which is parallel to the CCD. The apparent position of that edge can be accurately measured. For each such measurement, the CCD is stepped along its axis (the Leitz y–axis) so that the scans are taken at the same location on the MTF test chart. In this way, rotational misalingment of the test chart itself will not affect the results. In practice, accurate results can be obtained by choosing only 50 pixels spread along the CCD, and stepping them over the edge in 30 steps each of 4μm intervals. This scheme is implemented in the C program `xscan2`. The output file generated should look like Figure 5.4 when viewed with `displaysc`. The image contains information from all regions of the scan, not just the chosen edge, and hence the required part of the data needs to be extracted into a new, smaller image file. This is done using the program `xextract`. If displayed, this image should simply comprise a horizontal edge. The relative positions of each of the 50 chosen pixels can then be determined using the program `ypositions`, relative to the mean position defined by choosing a representative range of pixels – say pixel samples 26 to 35 (*i.e.* the central $\sim 20\%$ of the CCD). Those relative positions can be plotted using the program `shift_read` (see Figure 5.5), and the amount of bridge rotation can be obtained by fitting a straight line to that data, as done by program `rotfit`. Note that optical distortion effects are present towards the low pixel number end of the CCD; these should be excluded from the

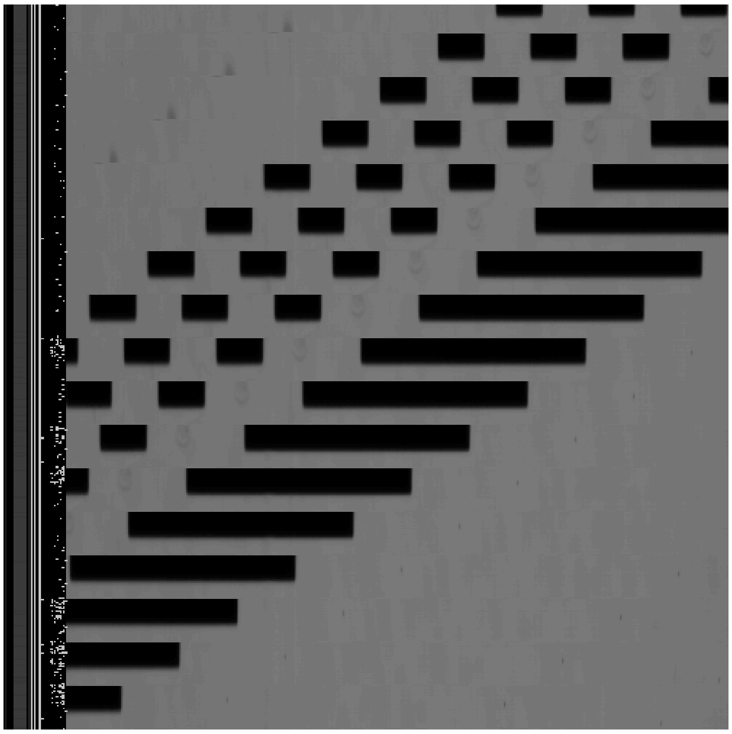

Figure 5.4: Displayed output from **xscan2** (only the first 500 × 500 pixels of the image are shown here).

fitting process as in the example below. The bridge rotation should be adjusted so that the residual positional errors are as small as possible (say a few tenths of a micron). Then, the residual errors (due to rotation too small to be adjusted for by the micrometer and any optical distortion) are removed via a polynomial fit to the residual errors as a function of image position on the CCD (see Section 6.7). A typical command sequence might be as follows (continuing from Section 5.2.4):

```
cosaxp0> xscan2 202.800 329.24995 394.95 xscan.dat
...
cosaxp0> displaysc xscan2.dat
scan length is      2090 : range of pixel numbers to use ? 1 500
number of scans is  1500 : range of scan numbers to use ?  1 500
...
cosaxp0> xextract xscan2.dat
scan length is      2090 : range of pixel numbers to use ? 1 2090
number of scans is  1500 : range of scan numbers to use ?  1 1500
output filename ?                               xextract.dat
pixel number [45] ? 45
number of scans per frame [30] ? 30
sampling interval [40] ? 40
cosaxp0> ypositions xextract.dat
scan length is        50 : range of pixel numbers to use ? 1 50
number of scans is    30 : range of scan numbers to use ?  1 30
start and end pixels for mean profile ? 26 35
```

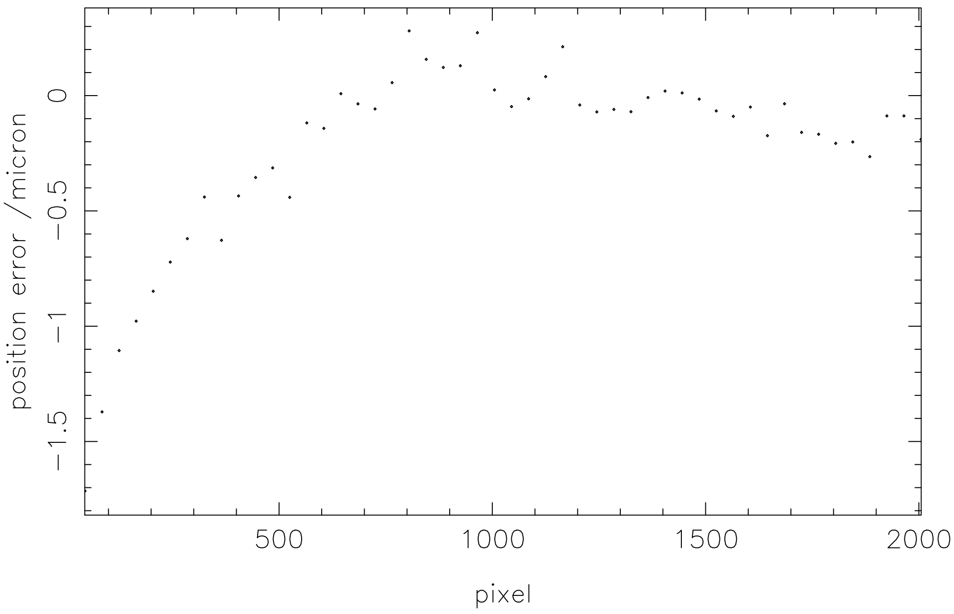

Figure 5.5: Displayed output from **shift_read** with input data from **xextract** and **ypositions**.

```
sampling interval (/mm) ? 0.004
output filename         ? ypos.dat
cosaxp0> shift_read
input filename ? ypos.dat
start & end pixel numbers ? 1 50
pixel interval ? [1]      40
first pixel number ? [1]  45
Graphics device/type (? to see list, default xwindows):
xwindows
cosaxp0> rotfit
input filename ? ypos.dat
Graphics device/type (? to see list, default xwindows):
xwindows
start & end pixels for fit ? 14 45
solution coefficients ....
  1.50802713926355      -5.111001000965938E-002
tan(theta) =    -0.1278E-03 assuming 400 micron sampling
micrometer moves 0.04 mm anticlockwise
```

5.2.6 Adjustment of bridge rotation

The bridge rotation adjustment is extremely delicate, and only with practice is it possible to achieve the desired accuracy. The micrometer gauge located up on the right–hand side of the y-axis assembly is accessed by standing on the machine's granite bed (**not** the x-axis block) and removing the cowling. Relative adjustment only is provided for; looking at the micrometer from the front and adjusting clockwise allows measurement of the bridge rotation in the same sense when viewing from above. The adjustment calculated by `rotfit` (see the previous Section) is also in this same sense. Note that, as mentioned before, the micrometer adjustment is relative: one cannot simply move the micrometer to rotate the bridge. Two allen bolts lock the bridge in position; a spring mount is attached which pulls the bridge anticlockwise if these bolts are loosened. The micrometer can be used to touch the arm lever; taking the strain of the spring (strong fingers are needed!) and then releasing the allen bolts allows bridge rotation in either direction by the desired amount using the micrometer to measure the arm movement. **Never use the micrometer head to take the strain of the spring.** In outline, the procedure is as follows. Adjust the coarse micrometer scale to just touch the arm support, then lock the coarse scale. For an anticlockwise adjustment, turn the fine scale by the required amount (one complete revolution of the fine scale corresponds to 50μm of adjustment). Release one allen bolt; take the strain of the spring then release the other. Allow the arm to move until it just touches the micrometer head again, then tighten the bolts. After an adjustment, always release the coarse lock and move the micrometer head well away from the arm so that it is free to rotate and is not under any mechanical strain. A clockwise adjustment is similar, except that the arm has to be pushed against the pressure of the spring and the micrometer used to gauge the amount it has moved (once again, never use the micrometer head to push against the spring arm).

5.2.7 Measurement of magnification error

If the CCD is not lying precisely in the focal plane of the imaging lens, then there will be a resulting departure of magnification from unity. Ray–tracing for the imaging lens shows that an error in focal plane positioning of 1.7μm results in an error in magnification of 1 part in 10^5; measurements using the scripts and procedures described in this Section indicate a lower figure of 0.9μm for the same magnification error. If the CCD is too far away from the lens the measured image will appear larger than the true object being scanned. For a lane width of 1.5cm this would correspond to a pixel positioning error at each edge of a lane of 0.075μm. Since the CCD can be positioned to an accuracy of only about 20μm, the corresponding lane–edge error is of order 1μm. Furthermore, if the CCD lies parallel, but not in, the focal plane, then the magnification error is constant across the device, whereas in general the CCD will be tilted with respect to the focal plane and the magnification error will vary across a lane. Hence, the magnification error needs to be carefully determined when installing the CCD and eliminated as far as possible when adjusting the optical alignment. However, due to the design of the CCD camera, the device cannot be realigned without disturbing the imaging lens position and consequently the lens–CCD distance. This limits the level of accuracy that can be obtained in the measurement/adjustment loop, and results in the constant component of residual magnification being needed for scan–time and off–line corrections (*e.g.* see Section 6.7).

The magnification error is measured by stepping the table at small intervals along the length of the CCD (the Leitz y–axis), passing each pixel in turn over and edge which is perpendicular to the CCD. Measurement of the apparent displacement of the edge in the image with each successive scan, and comparing with the table movement, provides us with a relative measure of the image size compared with the object size. The raw data are collected by the C program `yscan`. This program steps the table at intervals of 2.5μm for a total of 9000 positions, and hence generates an image file of size 38Mbyte. In that image each of the edges in the target appear as diagonal lines whose slope is equal to the pixel size (10μm) divided by the sampling size (2.5μm) – see Figure 5.6. Any one of those edges can be straightened into a horizontal edge by the window–extraction program `dw` (the extent of the window to be extracted can be determined using the cursor option in `displaysc`). If the magnification is unity, that extracted edge should appear perfectly horizontal. Departures from unity can be determined by Fourier cross–correlating the edge positions, as done by the program `ypositions`. The output from that program can be displayed by program `shift_read` (see Figure 5.7) and analysed for magnification error by the program `magfit`. As stated above, it is likely that, not only is the CCD not lying in the focal plane of the imaging lens, but also that it is tilted with respect to that plane. In that case the magnification error will vary along the CCD and the values fit by `magfit` will follow a quadratic curve. The gradient at any point along that curve gives us the amount by which the CCD lies away from the focal plane at that particular position. During installation of a CCD, this analysis enables the amount of shim needed at the three CCD module mounting points to be derived. For the final correction factor, linearly extrapolate the output values from `magfit` to the middle of the CCD (say pixel 1024), as in the following example (again note the exclusion of pixels in the periphery of the field of view to avoid errors due to optical distortion):

```
cosaxp0> yscan 198.1 335.75152 394.95 yscan.dat
...
cosaxp0> displaysc yscan.dat
scan length is      2090 : range of pixel numbers to use ? 1 500
number of scans is  9000 : range of scan numbers to use ?  1 500
...
cosaxp0> dw
 name of data file ? yscan.dat
 scan length is      2090 : range of pixel numbers to use ? 1 2090
 number of scans is  9000 : range of scan numbers to use ?  1 9000
 output filename ?                                 dw.dat
 number of samples per pixel (must be integer) (4) ? 4
 x,y position of left edge of window ?             301 5
 x,y position of right edge of window ?            310 5
cosaxp0> ypositions dw.dat
scan length is      2090 : range of pixel numbers to use ? 1 2090
number of scans is    37 : range of scan numbers to use ?  1 37
start and end pixels for mean profile ? 1001 1100
sampling interval (/mm) ? 0.0025
output filename        ? ypos_dw.dat
cosaxp0> shift_read
input filename ? ypos_dw.dat
start & end pixel numbers ? 101 2090
pixel interval ? [1]      1
first pixel number ? [1]  1
Graphics device/type (? to see list, default xwindows):
xwindows
cosaxp0> nmagfit
 input filename ? ypos_dw.dat
 start & end pixels for fit ?       401 1800
 start & end pixel numbers for plot ? 101 2090
 Graphics device/type (? to see list, default xwindows):
 xwindows
 solution coefficients ....
  1.127601669978369E-002  0.269114323485974      -2.993178365498755E-002

 position error = 0 at pixel =      5495.5
```

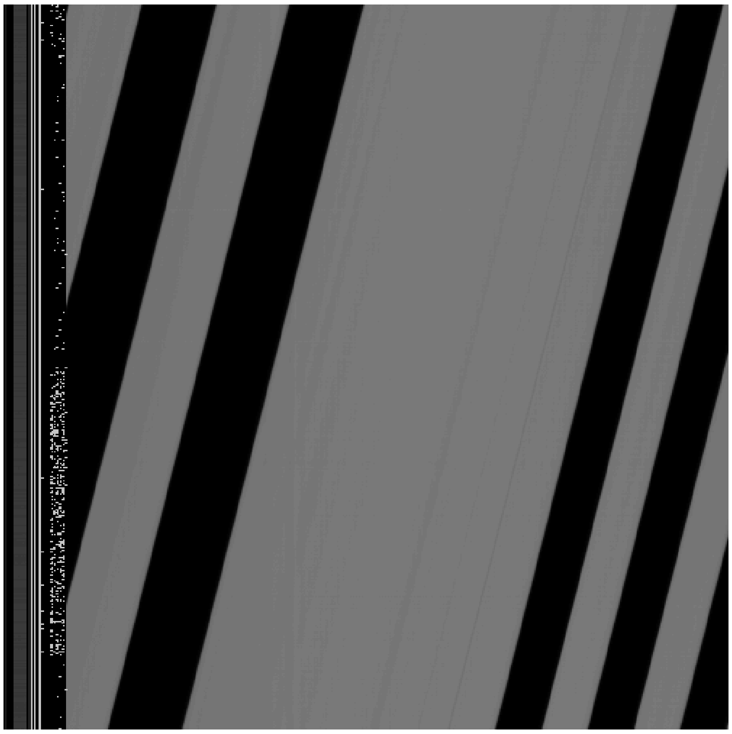

Figure 5.6: Displayed output from **yscan** (only the first 500×500 pixels of the image are shown here).

```
 magnification error at pixel 0 =        0.3290E-03

 magnification error at pixel 500 =        0.2990E-03

 magnification error at pixel 1024 =        0.2680E-03

  shims A (2 of) need to be increased by     36 micron
  shim B (1 of) needs to be increased by      4 micron
cosaxp0>
```

This measured value of α at pixel 1024 should then be used to create new versions of the correction files `xpoly.tcl` and `residual.corrns`. Section 6.7 describes the procedure that generates the other table geometry correction values in these files. If no change is necessary to those values (*i.e.* only the magnification factor is being altered) then execute as follows:

```
cosaxp0> axfit
         .
         .
         .
cosaxp0> resfit
         .
         .
         .
```

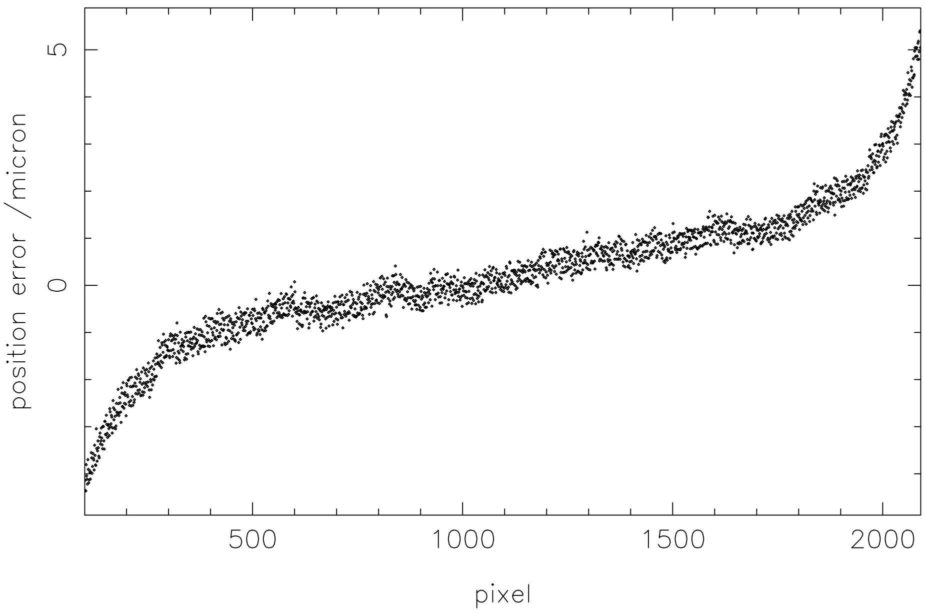

Figure 5.7: Displayed output from **shift_read** with input data from **diagonal_window** and **ypositions**.

5.3 Aligning and focusing the slit

Section 2.6 outlined the requirements for having a slit in the illuminating optics. This section describes how to align and determine the focus position for the slit. Realignment and/or refocusing should not be necessary unless the slit projection unit is disturbed or modified. Alignment is easily achieved using the available adjustments within the slit projection unit: slit rotation on the slit holder mount, and lateral displacement via the two micrometer adjusters on the 45° mirror below the illuminating lens. To align the slit, rotate so that the slit image is perpendicular to the CCD resulting in a few pixels being illuminated. Adjust either micrometer to get the illuminated pixels central (*i.e.* symmetrical about pixel 1024). The scripts `static` and `pixelplot` can be used to take CCD data and check where the illuminated pixels are. Then, rotate the slit by 90° and again adjust either micrometer to illuminate as much of the CCD as possible; small adjustments to the rotation should allow the entire CCD to be illuminated evenly.

To focus the slit, script `slitfoc` and program `slitfoctest` are available. The routines work along the same principles outlined in Section 5.2.3.

5.4 Changing the lamp

5.4.1 Safety considerations

Each lamp is supplied in a box containing safety instructions (read these if you are new to handling the lamps) and a plastic enclosure for protection. Since the lamps are prone to explosive failure, this plastic enclosure also protects the handler. It is recommended that goggles and gloves be worn when handling lamps (gloves also protect the glass envelope from finger marks). Never apply a torque to one electrode of a lamp while holding the other. Finally, carefully observe the polarity when installing a lamp, and ensure the power is off and the fan is stationary before opening up the illumination unit (see Section 1.10 for a brief description of the illumination unit). Note that the dust filter at the fan air intake on the illumination unit housing can become clogged with dust over a period of time. It is good practice to check the filter when changing the lamp (or at more frequent intervals if so desired) and tl vacuum clean the filter to ensure good air flow through the apparatus.

5.4.2 Lamp on/off procedure

When switching off an old lamp or switching on a new lamp, the following procedure should be strictly adhered to:

To power down:

1. Turn off 'LAMP ON–OFF' on the lock–in unit on left–hand side, then wait for 5 minutes.
2. Turn off 'FAN' on lock–in unit.
3. Turn off the Xenon lamp power supply (switch marked with white dot pushed in at blue marker position on large blue unit on LHS).
4. Turn off the Hall probe 5V PSU at the mains; plugs can then be removed from the wall sockets if desired.

[Note: you should not have to turn off 'MAINS ON–OFF' on the lock–in unit]

To power up: reverse the above procedure.

5.4.3 Installing a new lamp

The life of each lamp is limited to about 3 months of continuous operation, after which the electrodes will be eroded, the lamp output degraded by deposits on the inside of the glass envelope, and the lamps themselves become increasingly prone to explosive failure. To maintain light throughput and protect the ellipsoidal mirror it is a good general operating policy to change the lamp every 3 months. The following procedure should be closely adhered to when changing the lamp:

1. Switch off the light source as described above.
2. Remove the lamp housing (eight chrome plated screws), then the fan/cathode cover (two anodised screws) to gain access to both cathode and anode lamp conections.
3. Close the lamp housing shutter, lift the 45° cold mirror retaining clips and remove the cold mirror by sliding up. Gloves should be worn to avoid marking the surfaces of the mirror. Place the mirror in protective bubble–wrap on a flat surface away from any area where heavy items may be accidentally dropped.

4. Hold the upper electrode (anode) with the right hand and unscrew the vaned, knurled bolt with the left hand — be careful not to apply any torque to the lamp as the cathode is still firmly held. Lift off the copper anode connector.

5. Gently unscrew the lamp cathode by rotating at the cathode — **never** unscrew using the anode (upper) electrode! After a few turns the lamp will be high enough relative to the ellipsoidal mirror that the two–piece plastic cover can be replaced around the lamp and held by two gold twist–ties. Always cover the lamp as soon as possible to protect against glass shards in the event of explosive failure. Once covered, fully unscrew the lamp and lift out from the ellipsoidal mirror. Replace in its original box.

6. Take a new lamp carefully from its foam protection in the supplied box. Unscrew the small knurled nuts from each electrode. Place the lamp into position, carefully observing the polarity: the cathode and anode are clearly marked '−' and '+', 'down' and 'up' respectively — the cathode is the lower of the two connections in the lamp housing. After a few turns of the cathode (again, hold the lower electrode to screw in the cathode, never the upper) remove the plastic cover. Once this has been done, screw the cathode in finger–tight.

7. Place the copper anode connector on the anode screw–thread, then replace the knurled, vaned anode nut and tighten with the left hand while holding the lamp anode with the right hand. It cannot be emphasised enough how important it is **not** to apply any torque to the lamp envelope.

8. Replace the fan/cathode guard plate, replace the 45° cold mirror and close the lamp housing. Open the shutter on the lamp housing, switch on as described above. Replacement of the 8 chrome plated screws on the lamp housing can wait until the operation of the new lamp has been verified, but do not forget to finally secure the lamp housing on the unit.

The first thing to do after changing the lamp is to verify that the stability is within the required tolerance. Some Hamamatsu lamps have been found to be outside this requirement, and should not be used – see the next Section. After a lamp has been changed and stability verified, it may be necessary to make small adjustments at the gimble mount of the main fibre bundle on the illumination unit to attain a sufficiently flat–field (take a median flat — see Section 4.3.4 — to check the flatness of illumination). Any dramatic loss in throughput (*eg.* when compared with the previous lamp) should be investigated in conjunction with the alignment procedure detailed in the separate document describing the illumination unit and its set–up.

5.5 Measuring the stability of illumination

A script is provided in `/sdata/scos/checks/stability` to monitor the light level (via the reference channel) over a periods of $\sim$ 30s and output stability information on the terminal screen and laser printer (see Figure 5.8). It is good practice to check this frequently (say, at the beginning of each week) to ensure stable illumination and good throughput. Execute the script as in the following example:

```
cosaxp0> cd /disk1/scos
cosaxp0> source /sdata/scos/checks/stability
...
Maximum value =  5364 ADU
Minimum value =  5318 ADU
```

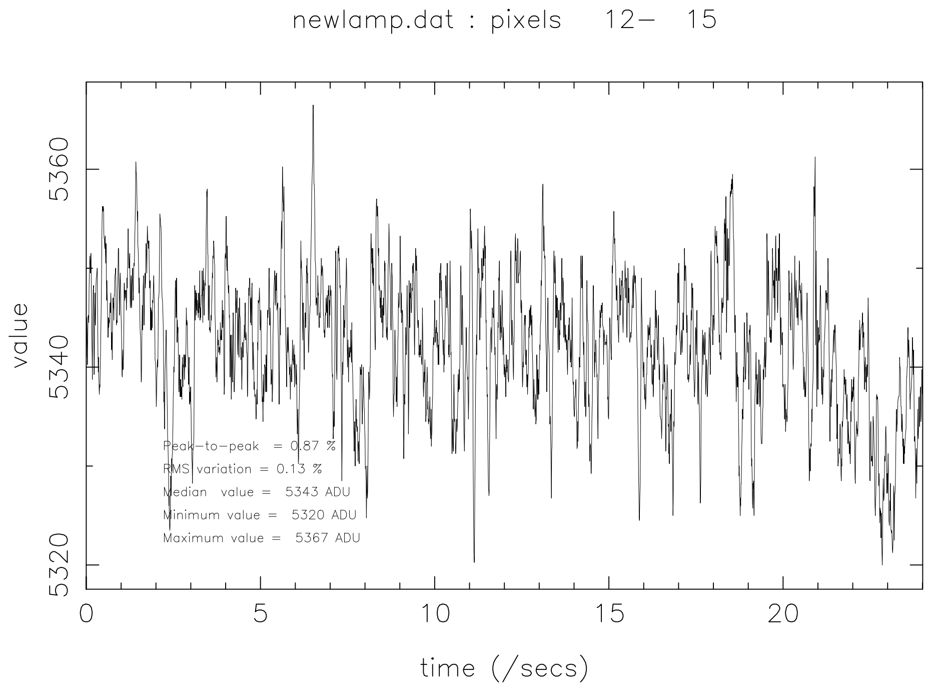

Figure 5.8: Displayed output from script **stability**.

```
Median value  =  5341 ADU
RMS variation =  0.13 %
Peak-to-peak  =  0.87 %
```

Typical figures should be $\sim 0.1\%$ RMS and $< 1\%$ peak-to-peak in order for low measurement noise and for the reference correction to work accurately. The reference channel is set up to yield ~ 5000 ADU — any significant difference from this value (say more than $\pm 20\%$) should be investigated.

5.6 Testing the optical system: resolution and point–spread function

The resolution and point–spread function (psf) can be measured using the MTF chart (strictly speaking the following derives a 'line–spread' function). Follow the procedure detailed in Sections 5.2.1 to 5.2.4 to set the machine, focus on the chart and locate an edge perpendicular to the CCD. Then, that edge may be scanned at different positions on the CCD, and therefore different positions in the imaging system field–of–view, using the commands `absmov` and `locate`. The vertical edge should not be aligned with the scan direction (in practice, non–alignment will generally be the case when loading the test chart into the plate holder). Then use codes `sc_to_ras` (FORTRAN source) to extract the edge data from the image, and `Apsf` (C code) to derive the psf as in the following example:

```
cosaxp0> absmov xyz _ _ _
```

```
cosaxp0> locate 500 edge.dat
cosaxp0> displaysc edge.dat
...
cosaxp0> sc_to_ras edge.dat
 scan length is      2090 : range of pixel numbers to use ? _ _
 number of scans is  9000 : range of scan numbers to use ?  _ _
 output filename ?    edge_ras.dat
cosaxp0> Apsf edge_ras.dat psf.dat
```

Note that the image obtained by `locate` must be displayed and the cursor used to measure a rectangular box containing the edge alone and no other features. The output file from `Apsf` is a plain text file that can be read into a subsequent plotting program, or which can be input into higher level plotting packages.

It is important that the resolution (in terms of the psf FWHM) is no larger than 12 to 15μm; furthermore, it is also vital that the psf has no systematic change in its shape across the field–of–view. Taking data from the same edge at say 10 positions across the CCD allows this to be checked; care should be taken to look for changes in shape in the low–level wings of the psf.

Chapter 6

Positional stability and accuracy

6.1 Introduction

The SuperCOSMOS system produces a two dimensional pixel map of the plate being scanned at 10μm resolution. Ideally, the image produced should be an exact 2–d representation of the photograph with square 10μm pixels — in principle, the image analysis software *assumes* that this is the case. Any random and/or systematic errors in the positions of the pixels or the position of the camera head during scanning will lead to corresponding errors in the positions of objects output by the image analyser; such errors would obviously affect the ultimate astrometric precision that can be attained from scanned photographs. Of course, Schmidt plates in themselves have systematic position– and magnitude–dependent errors present (*eg.* those due to distortion produced by the telescope optics or plate clamps). Discussion of such errors is beyond the scope of this manual but is irrelevant in any case; suffice it to say here that the design philosophy of the machine is that the measuring process should introduce as little additional random and systematic error to the data as possible. It is, however, important to discuss the fundamental limiting positional accuracy of a typical astronomical photograph.

6.1.1 Intrinsic astrometric accuracy of photographic emulsions

There have been a number of theoretical and empirical studies concerning the limiting accuracy with which one can centroid an image in a photographic emulsion (eg. Fresneau 1978, Auer & van Altena 1978, King 1983, Lee & van Altena 1983, Irwin 1985). The fundamental limit is set by the emulsion granularity and the variation in emulsion noise with density. Lee & van Altena (1983) – hereafter LVA83 – found that, provided the image size is large enough so as to be fully sampled by the imaging system, to first order the accuracy is proportional to the emulsion granularity for images of a given density (the increase in emulsion noise with density and saturation effects result in a limiting accuracy being approached as images become more dense). From LVA83 the ultimate grain noise limited positional accuracy with optimal sampling, $\sigma_{\rm X}$, is given by

$$\sigma_{\rm X} = \frac{c_0}{D_0^{1/2}} f(D_0/B), \tag{6.1}$$

where c_0 is a granularity constant, D_0 is the peak density of the image above sky background, B is the background density and f is a slowly decreasing monotonic function, $f = 2.37$ at $D_0/B = 1$ and $f = 1.31$ at $D_0/B = 10.0$ (the typical full dynamic range of a $B = 0.5$ density, fine grained photographic emulsion is around 5 densities). The quantity c_0 is related to the

Emulsion	Kodak diffuse granularity G^*	c_0 /μm	σ_X /μm	Example of emulsion use in sky survey†
103a	0.030	0.51	0.41	POSS–I blue/red
IIa	0.019	0.32	0.26	ESO–B
IIIa; IV–N	0.016	0.27	0.22	SERC–J/ER/I; ESO–R; POSS–II
Tech-Pan 4415	0.008	0.14	0.11	UKST Hα Survey‡

Notes:
* From 'Scientific imaging with Kodak films and plates', Kodak publication No. P–315.
† Morgan et al. (1992)
‡ Parker & Phillipps (1997)

Table 6.1: Limiting centroiding errors, for various photographic emulsions, predicted by the analysis of LVA83 assuming optimal sampling, zero measurement noise, background diffuse density of 1 and a peak diffuse density of 4.

Kodak diffuse granularity constant G via

$$c_0 = G\left(\frac{1810}{2\pi}\right)^{1/2}, \tag{6.2}$$

where 1810 μm^2 was the measuring aperture used by Kodak to determine G. Given a diffuse background density of 1.0 (typical of sky survey plates) and a bright image of peak density ~ 4.0, then $f \sim 1.6$ (Figure 1 of LVA83) and σ_X approaches a limit. Values of the limiting σ_X under such conditions with optimal sampling and assuming no additional measurement noise are tabulated in Table 6.1 for the common sky survey emulsions. Clearly, a high dynamic range machine having routine positional accuracy in each co-ordinate somewhat better than these σ_X values is required to extract all the positional information from the emulsion. In practice, this accuracy can only be attained using full, two–dimensional profile fitting (cf. LVA83); however, Irwin (1985) has shown that the difference in precision between profile fitted centroids and intensity weighted centroids (as calculated in the SuperCOSMOS image analysis software) is only significant for the faintest images (those where $D_0 \approx 0.1$ densities above sky background and $\sigma_X > 1$ μm for all emulsions).

6.2 Definitions and methodology

Following Miller (1992), we define two terms pertaining to the positional accuracy of the measuring machine itself:

- The *repeatability* is the accuracy to which measured positions can be repeated on successive measurements separated by long or short timescales. Good repeatability is important, for example when measuring relative positions on plates with the same field centres.

- The *absolute accuracy* is the accuracy to which a position can be measured with respect to a standard length. Good absolute accuracy is needed when measuring plates with different field centres (eg. POSS I/II) or when tying measurements in to a standard, global astrometric reference frame.

It follows that without good repeatability, it might not be possible to accurately measure and correct any systematic errors present in order to achieve good absolute accuracy — indeed, it might not be worth correcting systematic errors if random errors are present and dominant. Hence, good repeatability must be verified before attempting to measure any systematic errors In addition, we note that in any procedure that compares two measurements in order to determine absolute accuracy or repeatability, the standard errors on differences in position will be $\sqrt{2}$ times larger than the error in determining a position in a single measure (cf. Evans & Irwin 1995).

6.3 Factors affecting repeatability

In order of decreasing significance, the following should be considered when optimising machine repeatability.

6.3.1 Stability of the table during drift motion

Leitz PMM precision measuring machines were designed for use in a static mode in which a sensor probe touches the surfaces of the object whose dimensions are required. SuperCOSMOS operates in a drift mode, actioned by the low–level command `xdrift`, building up a plate measurement by raster scanning in lanes (and issuing one `xdrift` command per lane). As the granite blocks on the table move during a scan, the three air–cushioned feet that the machine is supported by compensate for the redistribution of weight: as a result, the table 'wobbles'. During a drift, a closed–loop algorithm checks the current Leitz y–axis reading against that at the start of the drift, and nudges the table back into position if it has wandered. Moreover, it is important that the Moiré fringe grating readers are correctly set up and the electronics adjusted so as to yield $\sim 0.1\mu$m relative accuracy as the table moves (*eg.* see Section 1.4). That set–up procedure is once more beyond the scope of this manual (Leitz technician Keith Baker should be consulted in the event of suspected problems in this area). We note here that without the closed–loop drift, repeatability errors of up to 10μm are observed; any incorrect set–up in the fringe grating readers can yield errors of order 1μm.

6.3.2 Temperature stability

It is vital that the chamber temperature remains constant for good repeatability. Any change in temperature would result in expansion or contraction of machine components (particularly critical are the fringe gratings) and of the photographic plate being scanned. For example, a 1°C rise in temperature results in 3μm expansion in the 0.5m length glass gratings. The temperature is therefore kept stable to ± 0.1°C to maintain repeatability at the level of $< 0.3\mu$m. Note that because adjacent areas of plate are scanned at different times with the lane raster scan employed, temperature variation would not simply produce a correctable stretch into the measured positions. A digital readout in the control room enables monitoring of the chamber temperature.

6.3.3 Mechanical stability

Any mechanical perturbation during a plate measurement may result in repeatability errors. The air cushioned feet on which the machine sits damp out any vibration transmitted through the chamber floor. On the machine itself, the plate holders should be firmly clamped onto the Leitz x–axis carriage, while the spring–loaded plate holders must firmly grip the plate. Finally, it is vital that the air pressure supplied to the machine remains above $\sim$ 6 bar and that fluctuations in the pressure above that value as the compressors switch on and off are damped by the reservoir tanks and regulators — repeatability errors of order $\sim 0.5\mu$m were observed on the original system before installation of an extra air reservoir and pressure regulator next to the machine.

6.3.4 Stability of illumination and reference correction

Good repeatability can only be achieved if the illumination system provides light levels stable to $< 0.5\%$; in addition it is vital that the reference correction works accurately. Section 5.5 details the procedure for measuring the stability of the light source, while Section 4.4 demonstrates how to verify that the reference correction is working accurately.

6.4 Measurement of repeatability performance

There are two methods for checking the repeatability performance of the table. The first is relatively quick, and is useful when adjusting the `xdrift` corrections or the electronics on the machine to optimise repeatability. The second allows a check over the full area of a plate scane and requires two measurements of the same plate; consequently, this second method takes much longer, but is a more complete and stringent test of the machine's performance.

6.4.1 Quick repeatability check

The quickest way to check the repeatability is to use the GUI system to scan a single lane of an astronomical plate twice without removing the plate (look in the directory `/sdata/scos/queue` for an appropriate job–spec file). Then, program `lxc` can be used to plot the differences in position of features (generally the emulsion granularity) between the two scans. The method adopted is to use fast Fourier transform cross–correlation of ranges of pixels, and it is accurate enough to show repeatability errors down to $\sim 0.1\mu$m.

Alternatively, if GUI operation is not available or convenient, data may be obtained using low–level scripts (*e.g.* `locate`, Section 2.8). If two strips of data are obtained in this way, then the program `lxc` can easily be modified to calculate and plot the results.

6.4.2 Full repeatability check

A full–plate repeatability check can be done by scanning the same plate twice and comparing the results for internal consistency. The script `/sdata/scos/checks/repeatability` is available for this purpose. Simply edit in appropriate values at the start of this script once the measurements and processing of the two plates are complete, then:

```
cosaxp0> source /sdata/scos/checks/repeatability
...
```

Plots will be produced from the laser printer in the computer room showing an array of 'lollipop' vectors indicating mean repeatability errors on scales of $\sim$ 1cm as a function of table position (*eg.* see Figure 6.1). Also plotted will be histograms of the x and y values of the repeatability errors (Figure 6.2). Typical RMS values of the repeatability should be $< 0.1\mu$m.

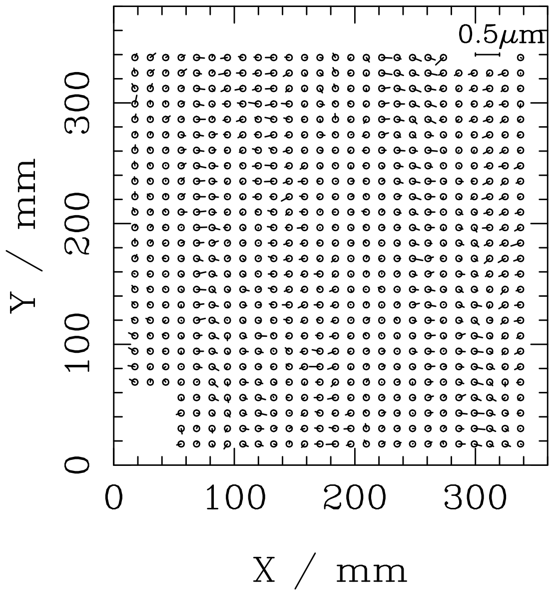

Figure 6.1: Vector diagram showing a comparison between two measurements of the same plate. Blank areas in the upper right and lower left of the figure are due to calibration step-wedges on the plate.

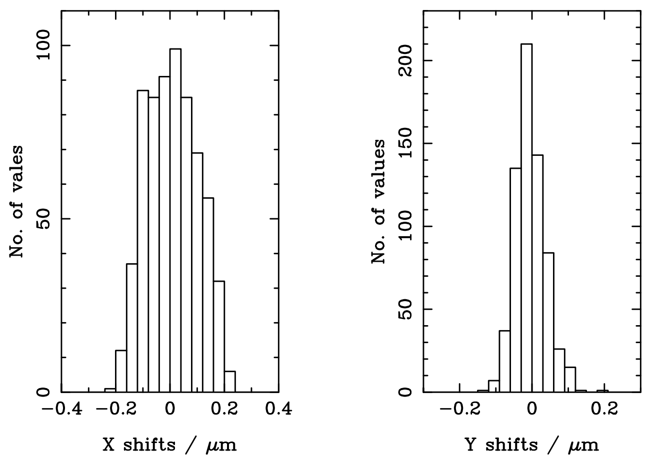

Figure 6.2: Histograms of x and y shifts from Figure 6.1.

6.5 Factors affecting absolute accuracy

Given good repeatability, the following give systematic errors, in approximate order of decreasing significance, affecting absolute accuracy:

6.5.1 Orthogonality of the xyz axes

Although the Leitz PMM 654 is engineered with sub–micron precision metrology as its goal, the orthogonality of its xyz axes can only be guaranteed to certain precision. In its normal static operating mode, software look–up tables would be used to correct for the measured non–orthogonality of its xyz axes. As stated previously, these LUTs are switched off for operating in drift–scan mode, hence new LUTs must be derived if a true cartesian co–ordinate system is required. The largest component of systematic error due to non–orthogonality is a global shear between the x and y axes of order $\sim 10\mu$m from one corner of the table to that diagonally opposite. Section 6.7 shows how this is measured and describes its correction.

6.5.2 Accuracy of the fringe encoders

The absolute accuracy of the xy table itself is of course limited by that of the encoding system used to position it. Again, these laser encoded gratings can only be constructed within certain tolerances, and low–level systematic errors are present which limit the absolute positional accuracy of the machine. Once again, the analysis described in Section 6.7 can solve for these errors, and shows how they can be eliminated to leave the xy table accurate at the desired level.

6.5.3 CCD alignment

Previouslt (Section 1.4) the raster scanning method of a SuperCOSMOS plate measurement has been described. Because the scan is built up as lanes with the pixels in the scan direction being defined by 10μm of table movement, it is vital that the CCD is as near to perpendicular to the scan direction as possible, and that there is little or no magnification by the imaging lens of the emulsion onto the CCD. Sections 5.2.5 and 5.2.7 describe how to minimise these errors and describe why it is not possible to eliminate them totally. Residual alignment error is removed in software in the final stages of image analysis. Residual magnification has to be taken into account during scanning (since the lane spacing will no longer be the scan length in pixels $\times 10\mu$m per pixel as it would be for unit magnification) so as to 'butt up' the lanes correctly; subsequently in the image analysis stage the axis parallel to the CCD must be demagnified by the same factor so as to leave the x and y axes of the measurement on the same scale. Section 6.7 describes how residual alignment errors and the magnification factor are incorporated into the scan–time and analysis–time correction files

6.5.4 Optical distortion, variable magnification and pixel placement in the FOV

The positional tolerances on the fixed geometry part of the scanning system (*i.e.* the imaging lens and CCD) are extreme. We would ideally require that there is no distortion or error in pixel placement leading to errors $> 0.1\mu$m; this means that CCD pixels have to be fabricated over a distance of 2cm at this level and that there be no distortion at a level greater than 0.005%. It was found that the full 2cm length of the CCD could not be used due to these tolerances being exceeded at distance from the optical axis around 6 to 7mm. Therefore, the scanlength is currently set at 11.52cm (or 1152 pixels). Optical distortions outside this range can easily be seen in the test data described in Section 5.2.7. Note also that it is necessary to get the illumination within this range as flat as possible (*i.e.* flat to the level of a few percent). This helps to reduce any systematic errors parallel to the CCD, and provides even image detection across the scanning lanes.

6.6 Derivation of the systematic error map

As discussed previously, the measuring machine has small residual systematic errors in absolute positioning (for example, the xy coordinates are not precisely orthogonal which results in a global shear in the xy positions output from the machine).

Let the systematic error map of the measuring machine be denoted by e^x_{ij} and e^y_{ij} where the measuring area is divided into a square grid of regions $i, j = 1$ to N. Then,

$$x_{\rm meas} = x_{\rm true} + e^x_{ij}; \tag{6.3}$$

$$y_{\rm meas} = y_{\rm true} + e^y_{ij}. \tag{6.4}$$

Furthermore, we will assume that we can decompose the error in x and y into the sum of two independent functions of x and y only:

$$e^x_{ij} = a_i + b_j, \tag{6.5}$$

$$e^y_{ij} = c_i + d_j. \tag{6.6}$$

This is similar to the approach used for calibrating out systematic errors from the APM machine (Evans & Irwin 1995). If an astronomical plate is measured in two orientations, one measurement made by rotating the plate 90° clockwise with respect to the coordinate system, then the positions of all the stars in the $i^{\rm th}j^{\rm th}$ region can be transformed back to the system of the original measurement and a mean zero-point shift in x and y will be present (after the global rotation and translation) due to the systematic errors. By *subtracting* the transformed co-ordinates of all the stars in a small ($\sim$ 1 cm square) region at point i, j from those in the 0° case we measure

$$\Delta x^{90}_{ij} = a_i + b_j + c_{i'} + d_{j'} \tag{6.7}$$

$$\Delta y^{90}_{ij} = c_i + d_j - a_{i'} - b_{j'}, \tag{6.8}$$

where box ij appears at position $i'j'$ in the rotated measurement. For a single rotation, we thus have $2N^2$ equations and $4N$ unknown error values. Since there are more equations than unknown variables, we can adopt a least–squares approach to obtain an estimate of the unknown error values. We can write the system of equations in matrix form:

$$\mathbf{C}.\mathbf{v} = \mathbf{m}, \tag{6.9}$$

where $\mathbf{C}$ is a sparse, rectangular matrix of $4N$ columns by $2N^2$ rows containing elements $C_{kl} = 0, -1$ or $+1$; $\mathbf{v}$ is the vector of $4N$ unknown values a_i, b_j, c_i and d_j; and $\mathbf{m}$ is the vector of $2N^2$ delta measurements. The solution of this equation may be obtained via an iterative scheme; however it is more robust to apply the method of least-squares to the system to obtain a filled, square matrix. We have a system of equations as follows:

$$\sum_{i=1}^{4N} C_{ki} v_i = m_k, \;\; k = 1 \text{ to } 2N^2. \tag{6.10}$$

This is solved by standard least–squares as follows: suppose we have a trial solution $\hat{v}_i$; then $\hat{m}_k = \sum_i C_{ki}\hat{v}_i$ and the sum of the squares of the residuals from this trial solution is

$$S^2 = \sum_k (m_k - \hat{m}_k)^2. \tag{6.11}$$

For the $n^{\rm th}$ value of v_i we require to minimise S^2, so

$$\frac{\partial}{\partial \hat{v}_n}[S^2] = 2\sum_k (m_k - \hat{m}_k)C_{kn} = 0, \tag{6.12}$$

or

$$\begin{aligned} \sum_k C_{kn} m_k &= \sum_k C_{kn}\hat{m}_k \\ &= \sum_k C_{kn} \sum_i C_{ki}\hat{v}_i \\ &= \sum_i \hat{v}_i \sum_k C_{kn} C_{ki}, \end{aligned} \tag{6.13}$$

which is a system of $4N$ equations in the solution $\hat{v}_i$. Writing $A_{ni} = \sum_k C_{kn}C_{ki}$, $b_n = \sum_k C_{kn} m_k$ and $x_i = \hat{v}_i$ equation 6.13 becomes

$$\sum_{i=1}^{4N} A_{ni} x_i = b_n, \;\; n = 1 \text{ to } 4N, \tag{6.14}$$

or as a matrix equation

$$\mathbf{A.x} = \mathbf{b}, \tag{15}$$

where $\mathbf{A}$ is a symmetric matrix ($A_{ij} = A_{ji}$). However, because the system of equations is formed from sets of difference measurements, it is degenerate in that some forms of translation error in the map of systematic errors are eliminated from the equations, so that no unique solution is possible. The simplest example of the degeneracy is a global translation error, which clearly would cancel out in the equations above, but other more complicated patterns also cause the matrix $\mathbf{A}$ to be singular. Despite this, we can still find a solution to the problem if we note that the set of possible solutions do not all have equal prior probability: we can choose the solution which minimises the residual $|\mathbf{A.x}–\mathbf{b}|$ following the approach described by Press et al. (1989). The technique involves singular value decomposition of $\mathbf{A}$; subsequently any vanishingly small singular values are set to zero and a least squares solution found (for a full discussion see Press et al. (1989) §§ 2.9 and 14.3).

6.6.1 Plate measurements and calculation of delta values

In order to measure delta values from the scans, a global plate map is required that rotates and zero-point shifts the xy coordinate system of one measurement onto that of the other. Subsequently, delta values may be obtained by small-scale linear least-squares models between the IAM intensity weighted centroids of all objects within a small region, or alternatively via pixel cross-correlations where the emulsion granularity generally provides the signal in the cross-correlations. Although the latter is likely to be more accurate, it is very time consuming and demands large amounts of disk storage (two mapping mode scans being needed online at a time). Experiments carried out show that the IAM method is sufficiently accurate – eg. the delta values being measured typically have values of order 1 μm while in Section 6.9.1 we show that the RMS measurement errors (ie. those resulting from the machine alone) in a single coordinate is $< 0.5\mu$m per object for the magnitude range used. Since each region typically contains several hundred objects defining the local linear model, the standard error in the delta values should be $< 0.05\mu$m. It is subsequently shown in Section 6.9.2 that the errors on the plate (ie. those resulting from emulsion noise) are dominant.

Note that in principle additional measurements at 180° and 270° plus reflections in y, x and about $y = x$ and $y = -x$ can be made to provide a more accurate solution; however tests show that this is not necessary given data from a IIIa–F emulsion at 0° and 90°. Should they be included, equations for those transformations would be as follows:

$$\Delta x_{ij}^{180} = a_i + b_j + a_{i'} + b_{j'}$$

$$\Delta y_{ij}^{180} = c_i + d_j + c_{i'} + d_{j'}$$

$$\Delta x_{ij}^{270} = a_i + b_j - c_{i'} - d_{j'}$$

$$\Delta y_{ij}^{270} = c_i + d_j + a_{i'} + b_{j'}$$

$$\Delta x_{ij}^{-x} = a_i + b_j + a_{i'} + b_{j'}$$

$$\Delta y_{ij}^{-x} = c_i + d_j - c_{i'} - d_{j'}$$

$$\Delta x_{ij}^{-y} = a_i + b_j - a_{i'} - b_{j'}$$

$$\Delta y_{ij}^{-y} = c_i + d_j + c_{i'} + d_{j'}$$

$$\Delta x_{ij}^{y=x} = a_i + b_j - c_{i'} - d_{j'}$$

$$\Delta y_{ij}^{y=x} = c_i + d_j - a_{i'} - b_{j'}$$

$$\Delta x_{ij}^{y=-x} = a_i + b_j + c_{i'} + d_{j'}$$

$$\Delta y_{ij}^{y=-x} = c_i + d_j + a_{i'} + b_{j'}.$$

6.7 Procedure for measurement and correction

In order to measure the current table geometry errors, the existing corrections should be switched off:

```
cosaxp0> cd /sdata/scos/machine
cosaxp0> mv table.corrns table.corrns.old
cosaxp0> mv xpoly_Full.tcl xpoly_Full.tcl.old
cosaxp0> mv xpoly_MagErrOnly.tcl xpoly_MagErrOnly.tcl.old
cosaxp0> mv residual_Full.corrns residual_Full.corrns.old
cosaxp0> mv yoptdist_Full.corrns yoptdist_full.corrns.old
cosaxp0> cp zero.corrns table.corrns
cosaxp0> cp residual_Zero.corrns residual.corrns
```

Then, a new magnification factor and optical distortion coefficients should be derived (if required). The magnification factor should be incorporated into a file `xpoly_MagErrOnly.tcl`. For example:

```
cosaxp0> cd /sdata/scos/machine
cosaxp0> cat xpoly_MagErrOnly.tcl
#   Polynomial coefficients for converting from X corrdinates assuming
#   uniform 10micron pixels to actual X coordinates.
#   Where XC is true X coords and XP is pixel-derived coords,
#   XC = kxcos + axcos * XP + bxcos * XP**2 + cxcos * XP**3
#
set axcos "+1.000140000000000"
set bxcos "+0.0E+000"
set cxcos "+0.0E+000"
set kxcos "+0.0E+000"
cosaxp0>
```

where axcos $= 1 - \alpha$, (α being output by program `magfit` as described in Section 5.2.7):

```
cosaxp0> cd /sdata/scos/machine
cosaxp0> ex xpoly_MagErrOnly.tcl
.
.
.
cosaxp0> cp xpoly_MagErrOnly.tcl xpoly.tcl
```

For the optical distortion erros in y, run the code `yposerrfit`:

```
cosaxp0> yposerrfit
Input file? ypos.dat         # output from code ypositions
Output file? yoptdist.corrns
Range of points to fit? 1 50
 Graphics device/type (? to see list, default xwindows):
Order of fit? 5
cosaxp0> mv yoptdist.corrns /sdata/scos/machine/.
```

It is then necessary to log out and log in again before commencing plate measurements. In order to then derive the table errors, two sequences of two measurements each at 0° and 90° orientation are required to provide the necessary information. Note that a survey grade plate is recommended (plate J8008 is a good example), and the measurements must be performed using a plate holder that has been levelled as far as possible. Measurements should also be carried out with the plate supported by a clear glass platten and with a 'fixed z' focus map, *i.e.* no movements in z should be allowed as these lead to systematic errors in xy. See the SuperCOSMOS Operator's Manual for more details of plate measuring.

In what follows, the four measurements are assumed to called J8008a,b,c and d, with a,c at 0° and b,d at 90° orientation; data are held in `/disk1/scos/J8008a/.` etc. Measurements a,b can be taken with `xpoly.tcl` and `residual.corrns` set as above; measurements c,d should be measured once a,b have been analysed and `xpoly.tcl` and `table.corrns` changed as in the following example:

```
cosaxp0> source ~scosdev/v033/.login
cosaxp0> cd /disk1/scos
cosaxp0> xycopy
```

```
Input file?
J8008b/iam.srtrd
Output file?
J8008b/iamc.srtrd
cosaxp0> hdspoke HKFILE=J8008a/hkfile NAME='deblend.select' VALUE='CHILD'
cosaxp0> hdspoke HKFILE=J8008b/hkfile NAME='deblend.select' VALUE='CHILD'
cosaxp0> lanesort IAMFILE=J8008a/iam.srtrd IAM_OUTPUT=J8008a/iamsrt.srtrd
         HKFILE=J8008a/hkfile
cosaxp0> pairconv HSEKP=J8008a/hkfile INFILE=J8008b/iamc.srtrd
         OUTFILE=J8008b/iamcconv
cosaxp0> lanesort IAMFILE=J8008b/iamcconv IAM_OUTPUT=J8008b/iamcconv.srt
         HKFILE=J8008b/hkfile
cosaxp0> rm J8008b/iamc.srtrd
cosaxp0> rm J8008b/iamcconv
cosaxp0> brisel
File for input?
J8008a/iam.srtrd
File for output?
J8008a/bright.dat
Areal extent to search (xmin,ymin,xmax,ymax in mm):
0.0 0.0 400.0 400.0
Maximum area (pixels):
100000
end2
cosaxp0> brisel
File for input?
J8008b/iam.srtrd
File for output?
J8008b/bright.dat
Areal extent to search (xmin,ymin,xmax,ymax in mm):
0.0 0.0 400.0 400.0
Maximum area (pixels):
100000
cosaxp0> ptran > J8008a/ptran2ab.log
1 100 10000 50 1 1000 1 2
J8008a/bright.dat
J8008b/bright.dat
J8008a/8008_atob_2.dat
J8008a/8008_b_coeffs_a_2.dat
80081 80082
cosaxp0> pair2 > J8008a/pair_ab.log
J8008a/iamsrt.srtrd
J8008b/iamcconv.srt
J8008a/pairs_b.dat
16.22 1152 28 0.05
cosaxp0> tablexy > J8008a/tablexy_2_ab.log
J8008a/iamsrt.srtrd
J8008b/iamcconv.srt
J8008a/8008_b_coeffs_a_2.dat
J8008a/pairs_b.dat
```

```
16.22 338.78 6.22 338.78
28 28 3.0 100
28 1152000 1000000
-23000 -19000
cosaxp0> zpshift
Residual data filename?
J8008a/tablexy_2_ab.log
Output filename?
J8008a/tablexy_2_ab.log.zp
cosaxp0> errmap > J8008a/errmap_ab.dat
1
J8008a/tablexy_2_ab.log.zp
9.0
cosaxp0> cd J8008a
cosaxp0> errrot
Error map data filename?
errmap_ab.dat
No. of lanes?
28
Extent of scan in mm (min, max)?
16.22 338.78
Output file?
errmap_ab.dat.rot
cosaxp0> axfit        # NB the value of alpha must be edited into this prog
Error map data filename?
errmap_ab.dat.rot
No. of lanes?
28
Extent of scan in mm (min, max)?
16.22 338.78
Order of polynomial to fit:
3
Output file for coefficients:
axfit.log
cosaxp0> byfit
Error map data filename?
errmap_ab.dat.rot
No. of lanes?
28
Extent of scan in mm (min, max)?
16.22 338.78
Order of polynomial to fit:
3
Output file:
table.corrns
cosaxp0>
```

then the coefficients in the file `axfit.log` should be edited into the standard `.tcl` format and saved to a file `xpoly_Full.tcl`:

```
cosaxp0> ex axfit.log
```

```
.
.
.
:w xpoly_Full.tcl
:q
cosaxp0> cp xpoly_Full.tcl /sdata/scos/machine/.
cosaxp0> cp table.corrns /sdata/scos/machine/.
```

Now the system correction files are ready for the measurements c,d: log out and in again, then perform these two measurements. The procedure is then the same to derive the residual error map file `residual.corrns` down to, but not including, the command `errrot` above. Instead, proceed as follows:

```
cosaxp0> cd J8008c
cosaxp0> resfit
Error map data filename?
errmap_cd.dat
No. of lanes?
28
Extent of scan in mm (min, max)?
16.22 338.78
Order of polynomials to fit:
5 5 5 5
Output file:
residual.corrns
cosaxp0> cp residual.corrns /sdata/scos/machine/.
```

The xy systematic correction files are now in place, and routine measurement may commence.

6.8 Test plate material

Details of the Schmidt plates used to test the machine are given in Table 6.2. For the purposes of astrometric tests, survey–grade plate pairs were chosen as close as possible in epoch to minimise errors from stellar proper motions and as close as possible in airmass to minimise any differential position effects due to refraction. We restricted the selection to fields containing photoelectric calibration sequences so as to be able to show centroiding errors as a function of actual stellar apparent magnitude in the various passbands. Details of the calibration sequences can be found in Hatzidimitriou, Hawkins & Gyldenkerne (1989) for the 103a plates and Hawkins (1996) and references therein for IIIaJ and 4415 material.

6.9 Results

6.9.1 Absolute accuracy

By measuring the same plate twice, but this time at two different orientations (in this case 0° and 90°), we can check the absolute positional accuracy by using software to rotate one measurement back on to the co-ordinate system of the other and examining the shift vectors as before. This process provides an instantaneous measure of the absolute accuracy, provided that there are not

Plate number	Emulsion	Central diffuse density	Min. Image diameter / μm
J8008	IIIaJ	1.00	35
U305	103a–O	0.60	35
U963	103a–O	0.87	45
R16747 F	4415	1.08	25
R16754 F	4415	0.92	25
J16180	IIIaJ	1.28	30
J16183	IIIaJ	1.35	35

Table 6.2: UK Schmidt Telescope plate material used to test the machine.

variations in machine positioning between scans. Comparisons of error maps produced by this method over a period of time provide information on the long-term stability of the systematic errors.

Figure 6.3 shows the residuals, divided by $\sqrt{2}$ for a single measure, as a function of magnitude for a 0/90 pair of measurements of plate J8008. Obviously, plate orientation of the scans should not change the image parameters obtained, and this demonsrates the accuracy of centroid measurement by the machine. Contributions to the errors in such a test include sampling effects and the signal–to–noise ratio of the CCD pixel data.

Figure 6.4 shows the systematic errors as a function of position on the xy plane resulting from decomposition using the analysis presented in Section 6.6 with data from a $0°/90°$ comparison for J8008 before any systematic effects were corrected. The largest systematic error component is a global shear (due to non–orthogonality of the co-ordinate axes) of order several microns from one corner of the plate to the other. This 'error map' was rotated so as to maximise the corrections applicable at scan time – Figure 6.5 shows the a, b, c and d values as a function of distance along each coordinate. After corrections introduced to scan time control and image analysis software, a new $0°/90°$ pair of measurements was done and the same comparison is shown in Figure 6.6. The large systematic errors have been completely eliminated by this procedure. The histograms of shift vectors remaining are shown in Figure 6.7, and the single co-ordinate, single measure standard errors of these distributions are $\sigma_X = 0.15\mu$m and $\sigma_Y = 0.15\mu$m; once more, these are consistent with the absolute positional errors measured previously. We again emphasise that these are the intrinsic errors in absolute positioning of the machine, *not* those in centroiding individual objects. We also emphasise, however, that it is of course not possible to approach the limiting accuracies listed in Table 6.1 unless the machine errors are small enough that the dominant source of errors in centroiding are from the emulsion granularity.

6.9.2 Examples of relative astrometry from Schmidt plates

Given the intrinsic machine accuracy demonstrated above, it should be possible, in principle, to approach the limiting accuracies given in Table 6.1 provided the imaging system fully samples the image profiles and does not introduce any additional noise into the measuring process. In practice, these limiting accuracies will never be wholly achieved due to saturation effects and

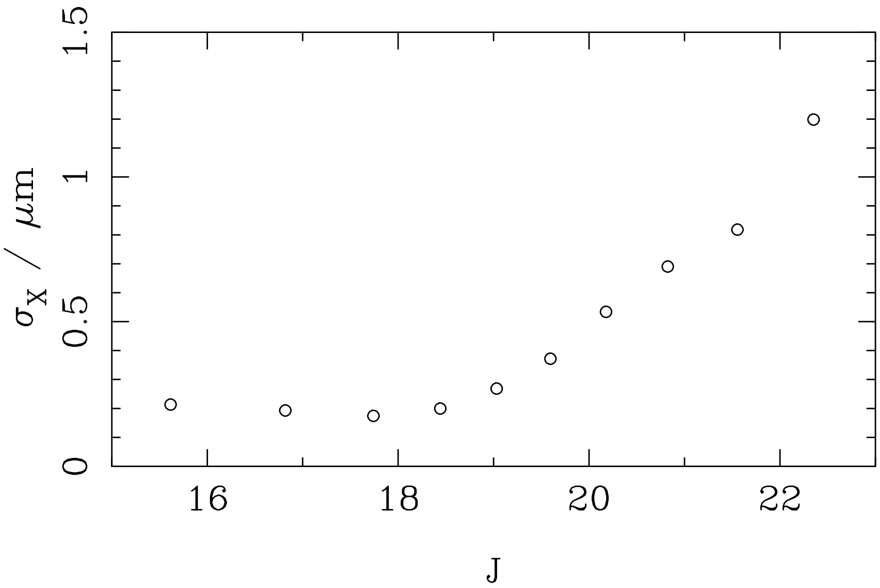

Figure 6.3: RMS centroiding error, as a function of magnitude, from measurements of the same plate in two different orientations

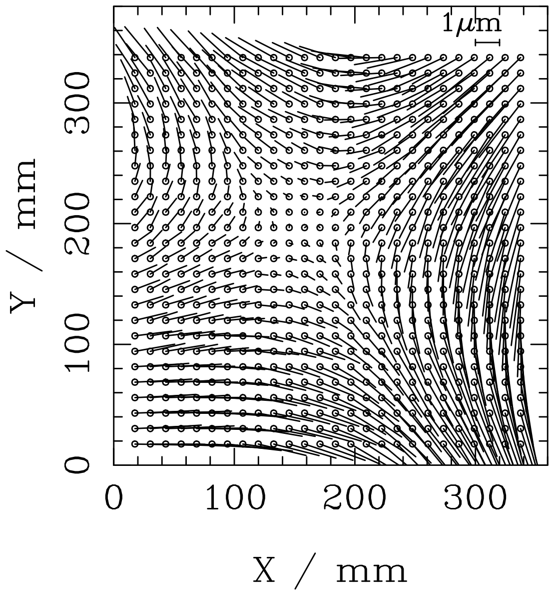

Figure 6.4: Vector diagram showing departures of the machines' xy from a true, rectilinear co-ordinate system before systematic correction.

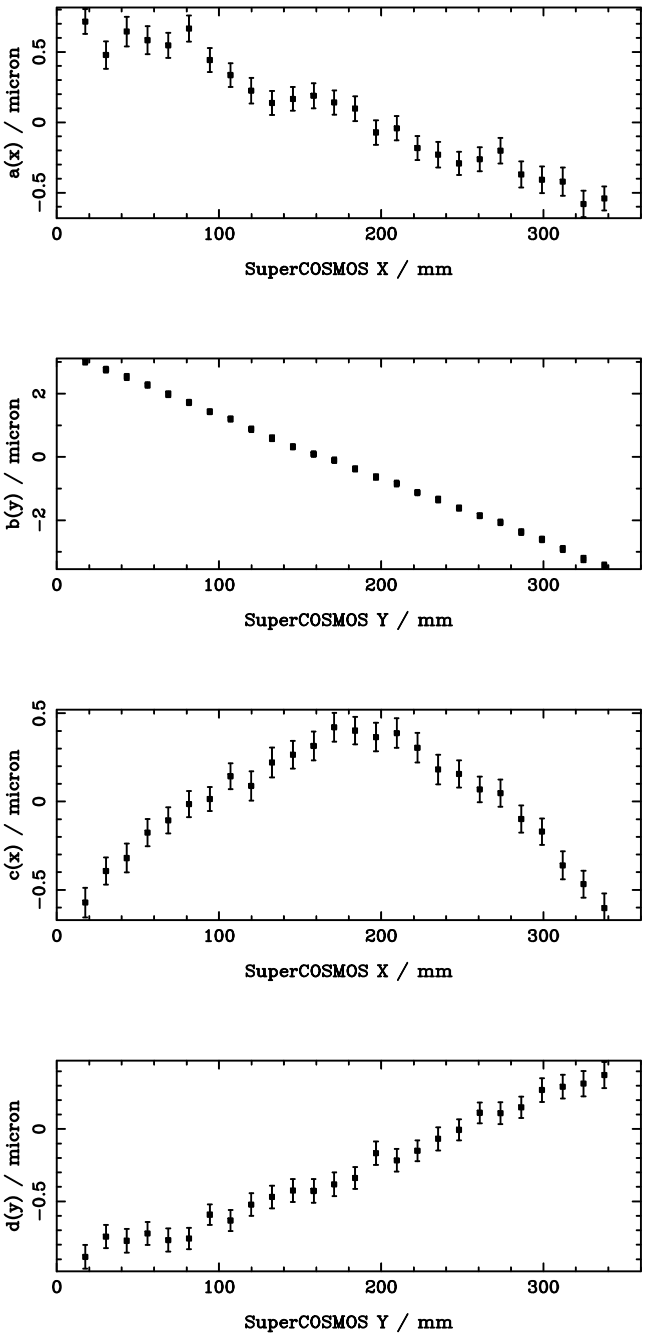

Figure 6.5: Error map decomposed as four independent functions: errors in x as a function of x, y and errors in y as a function of x, y.

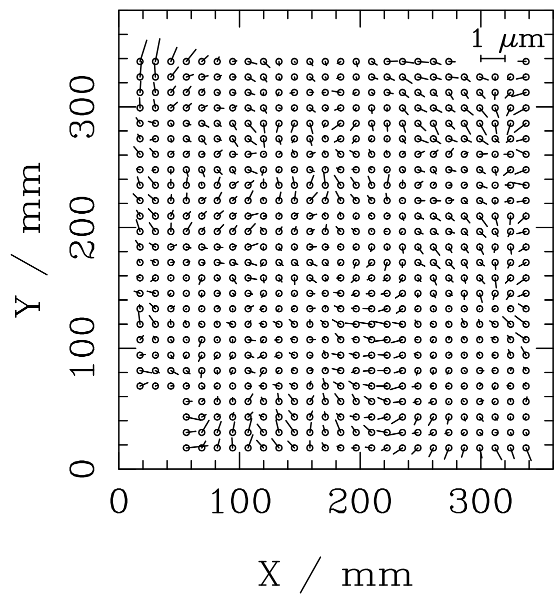

Figure 6.6: Vector diagram showing a comparison between two measurements of the same plate made at 90° relative rotation after systematic correction.

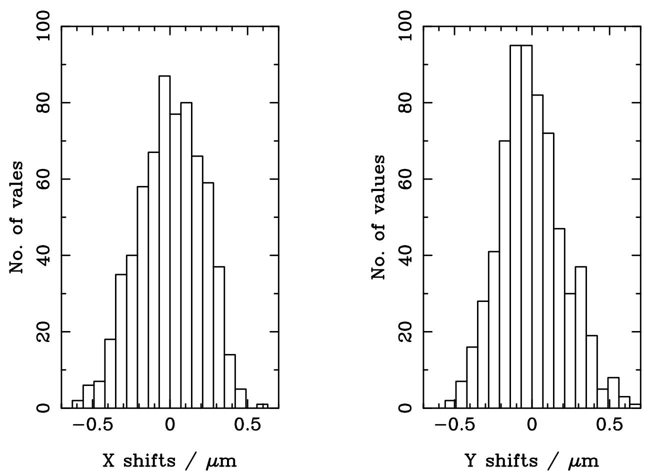

Figure 6.7: Histograms of x and y shifts from Figure 6.6.

image defects characteristic of Schmidt telescopes. We took the plate pairs detailed in Table 6.2 to test the astrometric performance with various emulsions. It is well known that over scale lengths of a few cm, emulsion stretch and plate deformation cause differential shifts in object position between two Schmidt plates of the same field (eg. Evans & Irwin 1995 and references therein); in addition there is in general a small magnitude dependent shift in centroids due to measurement of image structure caused by, for example, differential field rotation during exposure, aberrations in the Schmidt optics, scattered light in the emulsion, and image trailing during exposure (Wallace & Tritton 1979). Using a simple iterative scheme in small (~ 1 cm) boxes over the entire field, we applied a single linear least–squares model between object co-ordinates along with a residual magnitude dependent term to map out these effects and found the results illustrated in Figure 6.8 (iteration removes spurious object pairs and high proper motion objects not relevant to this study). The figures show the RMS residuals (median values from all $\sim$ 1cm boxes), as a function of magnitude, divided by $\sqrt{2}$ for a single measurement. Note that star/galaxy separation was carried out (using software and procedures described in Heydon–Dumbleton, Collins & MacGillivray 1989) to eliminate galaxies from this analysis, since such objects have centroiding errors up to twice as large as those for stars (eg. Irwin 1985).

6.10 Discussion

Figure 6.8 demonstrates the centroiding errors obtained for the three emulsion types 103aO, IIIaJ and 4415. In that Figure, the solid symbols represent the measurements (divided by $\sqrt{2}$ for the accuracy of a single measure). The data are plotted as a function of apparent magnitude in the left–hand panels, while in the right–hand panels the same data are plotted as a function of the peak specular density, D_0, of the images. This was derived by calculating

$$D_0 = \log_{10} \frac{T_{\mathrm{SKY}}}{T_{\mathrm{PEAK}}} \tag{6.15}$$

for all images to provide a mean calibration of D_0 versus instrumental magnitude, where T is the measured transmission. We assumed the Kodak granularity figures presented in Table 6.1; however these quantities are in diffuse density units and have to be scaled to the specular densities that the machine measures. Because of the telecentric lenses used in the imaging optics of SuperCOSMOS, the ratio of specular to diffuse density (known as the Callier Q factor) is large. We measured Q for the IIIaJ and 4415 emulsions in the diffuse density range 0.5 to 1.5 from the 16–spot KPNO step–wedge on the corner of the plates and found $\mathrm{Q}_{\mathrm{IIIaJ}} = 1.6$ and $\mathrm{Q}_{4415} = 1.45$. Unfortunately, no measurable wedge was available on the older 103aO plates, so we have somewhat arbitrarily assumed $\mathrm{Q}_{103\mathrm{aO}} = 1.7$ for this coarse–grained emulsion since Q is known to increase with increasing grain size. In fact, Q is also a weak function of density above 0.5D, but we have assumed constant Q for the sake of simplicity.

The solid curves in the right–hand panels of Figure 6.8 were calculated using the LVA83 analysis and the Kodak diffuse granularity figures in Table 6.1. We numerically integrated their equation 9 to calculate the quantity $f(D_0/B)$ in their equation 13 (equation 1 in this paper). Before comparison with our measurements, it is important to note that the LVA83 analysis is idealised in that the image profiles are assumed to be Gaussian and the effects of sampling are neglected. The analysis also assumes two–dimensional profile fitting of Gaussian functions to the image data. For our measurements, we should consider the following:

1. The SuperCOSMOS optics have a diffraction limited point spread function (psf) which in turn limits the dynamic range of the machine since the scanning system images a line of

pixels rather than illuminating a spot of emulsion as in PDS machines. This results in the transmission of high density pixels being affected by light from the wings of the psf — high density, high signal–to–noise cores of heavily saturated stars are not measured by this system, and the accuracy of centroiding will be less than that predicted in the LVA83 analysis. The light available to diffraction in the imaging lens is reduced using a 100μm air slit to illuminate the 10μm CCD pixels (the imaging system has unit magnification). Simple computations assuming an idealised Airy disk pattern show that the central density of an opaque 100μm object will be limited to $D_0 \sim 2.2$D — this is in good agreement with the densities measured from the machine for objects more than 4 mag above the plate limit (see Figure 6.8). For such objects, diffuse densitometer measurements of the relative intensity step–wedge imply $D_0 > 4$, as do measurements from PDS machines (eg. LVA83). Of course, the trade–off in this case is scanning speed — SuperCOSMOS images a line of $>$ 1000 pixels simultaneously in an integration time of 8ms, and therefore an entire Schmidt plate in ~ 2 hr. A change in slit width from 100μm to 25μm would theoretically yield another ~ 0.5D in dynamic range (provided such a thin slit were acceptable to other tolerances within the imaging system) and a potential increase in astrometric accuracy for images having $D_0 > 2.2$D.

2. The psf of the optics also causes intensity fluctuations between adjacent pixels to be correlated, so that we cannot simply estimate the emulsion noise from naive measurement of rms fluctuations between pixels. In our calculations we have adopted the nominal Kodak values for the noise sampled by independent 10μm pixels for each emulsion, which are larger than the measured rms fluctuations between pixels, and which should result in predictions of the uncertainties in image centroiding which are close to the measured uncertainties.

3. At high intensities the conversion from log(intensity) to density becomes highly non-linear and the density profiles of bright stars become significantly non-Gaussian, with flatter profiles near the peak. This results in the signal–to–noise ratio being *higher* in real images than in idealised images with Gaussian profiles *of the same peak density* (although not of course higher than would have been obtained without the non-linearity). Thus in theory the measured errors for bright stars should be smaller than the LVA83 predictions at a given value of D_0. However, as stated in (i), the limited dynamic range of the machine results in high density, high s/n data being lost.

4. The image positions are calculated by intensity weighted centroids rather than profile fitted centroids. We should expect, and Irwin (1985) has shown, that the errors from intensity weighted centroids are increasingly worse for fainter images.

5. For the smallest images typically attainable from U.K. Schmidt plates or films ($\sim 25\mu$m diameter) some aliasing of high spatial frequencies must occur, given the 10μm sampling of SuperCOSMOS. LVA83 tested their theoretical expectations with data in which the sampling interval was also only about one-third of the image diameter, obtaining results very close to their predictions, and hence it is likely that the finite sampling has little effect in our data also.

Bearing the above in mind, the agreement between measurement and theory in the right hand panels of Figure 6.8 is good for the 103aO and IIIaJ emulsions. However, for the 4415 film the measurement accuracy is poorer than expected. The origin of this discrepancy is not yet understood.

It must be emphasised that the accuracies illustrated in Figure 6.8 concern relative positions of stars with respect to stars within scales of a few cm on Schmidt plates. Tying measurements

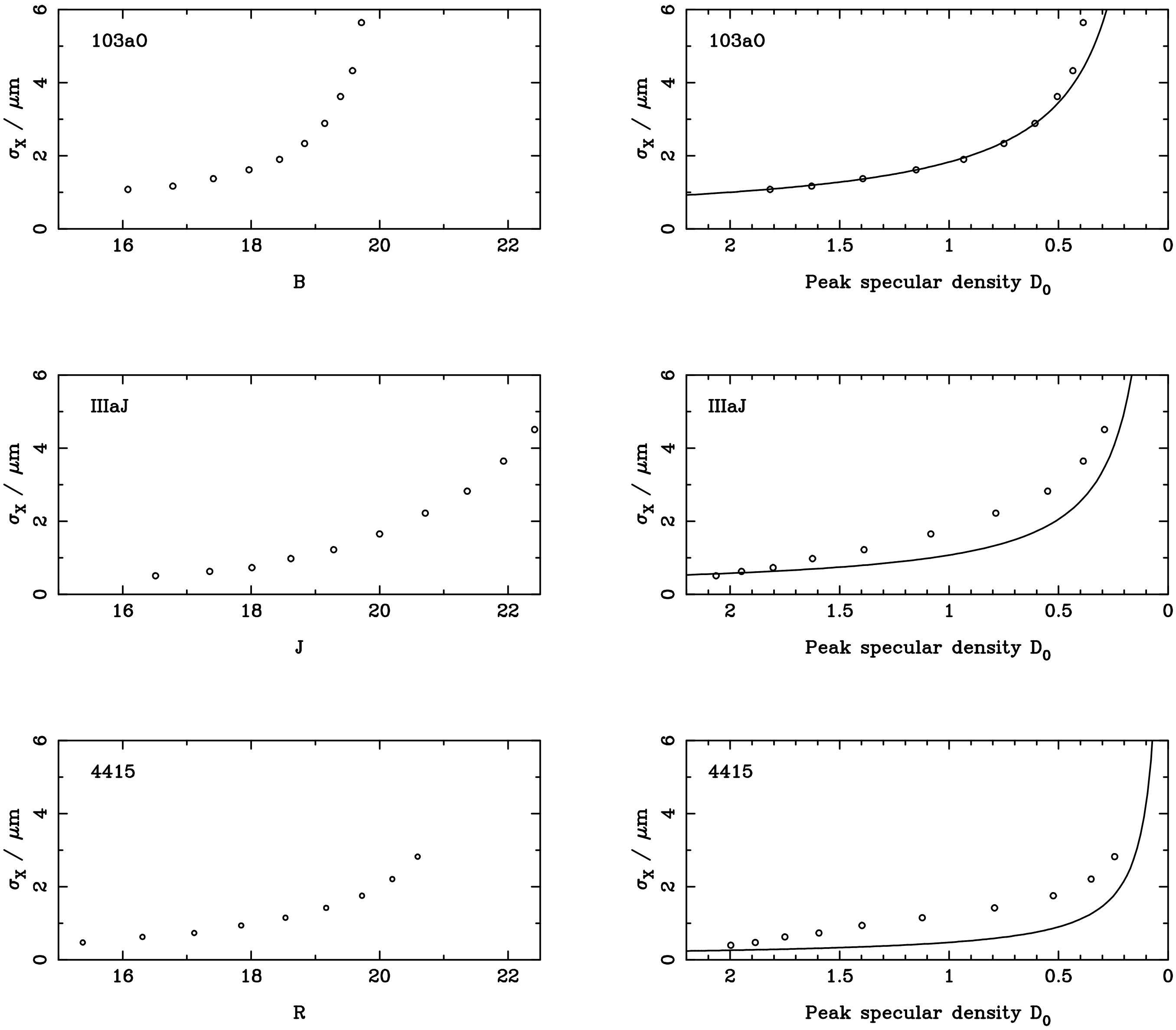

Figure 6.8: Plots of the RMS centroiding errors for various survey emulsions. The left hand panels show the data plotted as a function of apparent magnitude; the right hand panels are the same data in each of the three cases plotted in terms of the peak specular density of the images for comparison with theory (see text).

in to global astrometric reference frames, or indeed the fundamental zero proper motion frame defined by extra-galactic objects requires great care in deriving global astrometric solutions across the Schmidt plate and in the treatment of magnitude–dependent effects. Moreover, the accuracy obtainable is critically dependent on the quality of the plate material being measured and there is no guarantee that such precision is attainable from, for example, the large collection of private programme Schmidt plates available in the United Kingdom Schmidt Plate Unit plate library.

Bibliography

[1] Auer L.H., van Altena W.F., 1978, AJ, 83, 531

[2] Beard S.M., MacGillivray H.T., Thanisch P.F., 1990, MNRAS, 247, 311

[3] Epchtein N., et al., 1994, Ap&SS, 217, 3

[4] Evans D.W., Irwin M.J., 1995, MNRAS, 277, 820

[5] Fresneau A., 1978, AJ, 83, 406

[6] Hatzidimitriou D., Hawkins M.R.S., Gyldenkerne K., 1989, MNRAS, 241, 645

[7] Hawkins M.R.S., 1996, MNRAS, 278, 787

[8] Heydon–Dumbleton N.H., Collins C.A., MacGillivray H.T., MNRAS, 238, 379

[9] Irwin M.J., 1985, MNRAS, 214, 575

[10] Irwin M.J., 1992: see MacGillivray & Thomson (1992), p. 43

[11] Kent S.M., 1994, Ap&SS, 217, 27

[12] King I.R., 1983, PASP, 95, 163

[13] Kleinmann S.G. et al., 1994, Ap&SS, 217, 11

[14] Lee J-F., van Altena W.F., 1983, AJ, 88, 1683 (LVA83)

[15] MacGillivray H.T., Stobie R.S., 1984, Vistas in Astron., 27, 433

[16] MacGillivray H.T., Thomson E.B., 1992, Digitised Optical Sky Surveys, Astrophysics and Space Science Library Proceedings volume 174, Kluwer Academic Publishers

[17] Miller L., Cormack W.A., Paterson M., Beard S.M., Lawrence L., 1992, see MacGillivray & Thomson (1992), p. 133

[18] Morgan D.H., Tritton S.B., Savage A., Hartley M., Cannon R.D., 1992, see MacGillivray & Thomson (1992), p. 11

[19] Parker Q.A., Phillipps S., 1997, PASA, 14, 123

[20] Press W.H., Flannery B.P., Teukolsky S.A., Vetterling W.T., 1989, Numerical Recipes: The Art of Scientific Computing, Cambridge University Press

[21] Wallace P.T., Tritton K.P., 1979, MNRAS, 189, 115